SAND 2013-2766P

FY13 Q1 WATER POWER REPORT

FURTHER INVESTIGATION OF WAVE ENERGY CONVERTER EFFECTS ON WAVE FIELDS: A SUBSEQUENT MODELING SENSITIVITY STUDY IN MONTEREY BAY, CA

Submitted by

Water Power Technologies
Sandia National Laboratories
December 31, 2012

Jason Magalen, Grace Chang, and Craig Jones – Sea Engineering
and
Jesse Roberts – Sandia National Laboratories

Sandia National Laboratories is a multi-program laboratory managed and operated by Sandia Corporation, a wholly owned subsidiary of Lockheed Martin Corporation, for the U.S. Department of Energy's National Nuclear Security Administration under contract DE-AC04-94AL85000.

Contents

Figures

Tables

Introduction

To effectively generate commercial-scale power for an electric grid, Wave Energy Conversion (WEC) devices need to be installed in arrays comprising multiple devices to efficiently convert wave energy into electrical power onshore. The deployment of WEC arrays will begin small (pilot-scale or ~10 devices) but could feasibly number in the hundreds of individual devices at commercial-scale. As the industry progresses from pilot- to commercial-scale it is important to understand and quantify the relationship between the number of devices installed and the potential to effect the natural nearshore processes that support a local, healthy ecosystem. WEC arrays have the potential to alter near-shore wave propagation and circulation patterns, possibly modifying sediment transport patterns and ecosystem processes. As WEC arrays sizes grow, there is a potential for negative environmental impacts which could be detrimental to local coastal ecology, and social and economic services. To help accelerate the realization of commercial-scale wave power, predictive modeling tools are developed and utilized to investigate ranges of anticipated scenarios and evaluate the potential for negative (or positive) environmental impact.

The present study incorporates an industry standard wave modeling tool, SWAN (Simulating WAves Near-shore), to simulate wave propagation through a hypothetical WEC array deployment site on the California coast. Specifically, various sizes of WEC arrays are simulated to examine the changes to wave propagation properties (e.g. wave heights, periods and directions) in lee of the array in both the near- and far-field. Using and building upon results from a previous SWAN model sensitivity analysis (SNL, 2011), the study focuses on the change in wave properties resulting from variation in the ranges of SWAN model parameters, array geometries and array deployment locations (water depths).

At present, direct measurements of the effects of arrays on wave properties for a prototype scale WEC site are not available; therefore, the effects of varying model parameters on the model results must be evaluated before environmental assessments can be completed. The present study provides the groundwork for completing such assessments by investigating the sensitivity of the predictive model results to prescribed model parameters over a range of anticipated wave conditions. The understanding developed here will allow investigators to conduct predictive environmental assessments with increased confidence and reduced uncertainty in future phases.

Technical Approach

Model sensitivity analysis was conducted by Sandia National Laboratories (SNL) using the wave propagation model SWAN, developed by the Delft Hydraulics Laboratory. Of particular interest was to understand model behavior (i.e. alterations to wave heights, periods and directions) in the vicinity of point absorber WEC devices and device arrays. Although only point absorber-type devices are studied here, the fundamental description of resultant model behavior will be beneficial to the study of all classes of WEC devices.

Wave energy conversion devices will reflect and/or absorb differing amounts of wave energy depending upon device efficiency, device geometry, array configuration and local wave conditions. The devices are represented within the SWAN model framework as “obstacles” to the propagating wave energy; the model allows specification of wave energy reflection and transmission coefficients at each obstacle, which denote the fraction of wave energy that is reflected and/or transmitted. The energy that is not transmitted or reflected is “absorbed” by the obstacle.

Prototype WEC devices have varying absorption and reflection properties which are, at present, largely unknown, uncertain, or unreported. Model behavior based on varying reflection and transmission coefficients was the focus of a previous sensitivity analysis, where it was determined that the transmission coefficient variation had a much larger impact on leeward wave properties (SNL, 2011). Therefore, the focus of the model analysis described herein is to investigate further the effect of transmission coefficient variation along with additional model variations (number of WEC devices and WEC array deployment location [depth contour]).

Wave Model

As deepwater waves approach the coast, they are transformed by certain processes including refraction (as they pass over changing bottom contours), diffraction (as they propagate around objects such as headlands), shoaling (as the depth decreases), energy dissipation (due to bottom friction), and ultimately, by breaking. Since near-shore waves are the primary source of energy at the seabed in coastal settings, the accurate description of their propagation is a fundamental component in assessing near-shore circulation and sediment transport potential. The SWAN model has the capability of modeling all of these processes in shallow coastal waters.

The SWAN model is a non-stationary (non-steady state) third generation wave model, based on the discrete spectral action balance equation and is fully spectral (over the total range of wave frequencies). Wave propagation is based on linear wave theory, including the effect of wave generated currents. The processes of wind generation, dissipation, and nonlinear wave-wave interactions are represented explicitly with state-of-the-science third-generation formulations. Model boundary conditions can be explicitly specified by the user or may be obtained from nested, larger-domain modeling efforts (either SWAN or others such as WaveWatch III).

The SWAN model can also be applied as a stationary (steady-state) model. This is considered acceptable for most coastal applications because the travel time of the waves from the seaward boundary to the coast is relatively small compared to the time scale of variations in the incoming wave field, the wind, or the tide. SWAN allows for numerous output quantities including two dimensional (frequency and direction) spectra, significant wave height, mean wave period, mean wave direction and bottom orbital velocities (due to wave oscillations). The SWAN model has been successfully validated and verified in laboratory and complex field cases elsewhere, and, as mentioned above, was determined acceptable for evaluation at this location as well (Booij et al., 1996).

The selected modeling site was near-shore Monterey Bay and Santa Cruz, California. A previously validated SWAN model for the same region was used to propagate waves from deepwater offshore to shallow water (Chang et al., 2010 – unpublished). An offshore, coarser resolution grid model domain was nested with a finer resolution grid, near-shore model domain.

The model was in the Monterey Bay region using NOAA National Data Buoy Center (NDBC) buoy data from within, and in proximity to, Monterey Bay. Several local NOAA NDBC buoys provided measurements of significant wave heights, dominant wave periods, peak wave directions, wind speeds and wind directions at the buoy locations dating as far back as 1987. These measured datasets were then compared to model output to demonstrate excellent model performance.

The two SWAN model grids (coarse and finer resolution) were nested to predict the propagation of deepwater waves from offshore of Monterey Bay, CA, to near-shore Santa Cruz, CA. The coarse-grid (herein referred to as the Monterey Bay model domain) resolution was approximately 0.001° degrees in latitude and longitude (approximately 100 m grid spacing in x and y). The model was run

as a stationary model: meteorological and hydrodynamic conditions at the offshore boundaries were kept constant. Directional wave energy spectra conditions were exported from the coarse resolution model and used as boundary conditions for the nested, fine resolution model (herein referred to as the Santa Cruz model domain).

The grid resolution of the nested Santa Cruz model domain computational grid was approximately 0.00025° degrees in latitude and longitude (approximately 25 m in x and y). The wave spectrum boundary conditions were applied along the offshore boundaries of the Santa Cruz SWAN model domain. The nested grid model was also implemented as a stationary model.

The Monterey Bay and Santa Cruz SWAN model domains are shown in Figure 1. NOAA National Data Buoy Center (NDBC) buoys within the domain, used for validation, are noted in the figure. Data from buoy 46042 was used to derive Monterey Bay domain boundary conditions. Data from buoy 46236 were used to validate the model predictions for wave height, wave period and mean wave direction. Wave model validation is discussed in Chang, et al., (2010, unpublished).

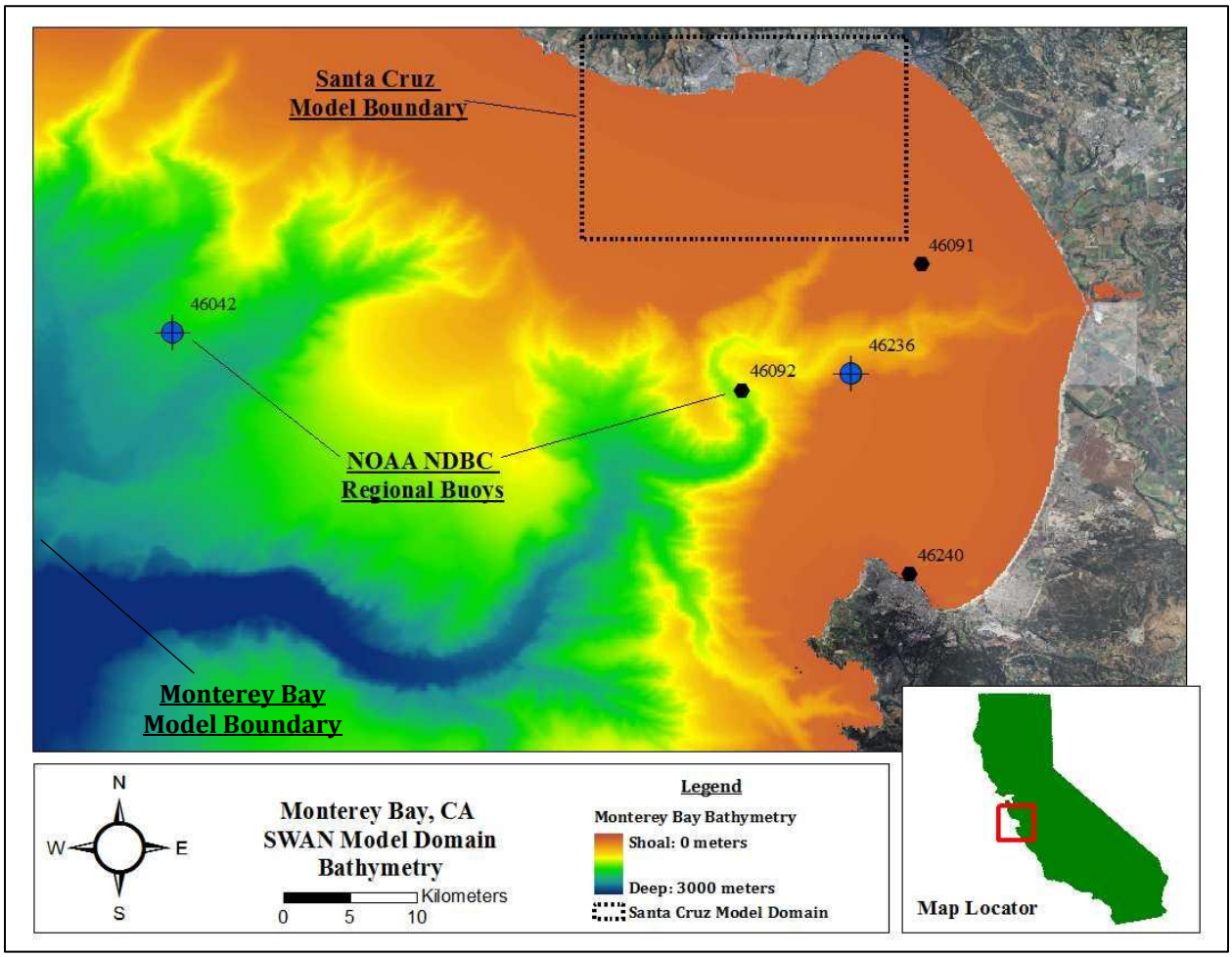

Figure 1. Monterey Bay and Santa Cruz, CA, SWAN model domains. Also shown are validation buoy locations.

Model Setup

In the present analysis, the device arrays were arranged in a honeycomb/diamond shape as a representative configuration (Figure 2). For simplicity, and to demonstrate model utility, each WEC

device was assumed to have a diameter of one grid cell (in this case, 25 meters). This ensured that the device effect on wave properties was represented in the model (in SWAN, obstacles must cross the direct line connecting two grid points in order to be represented in the model as a distinct obstacle). WEC devices were simulated in the model with 6-diameter spacing between devices, center to center. Devices were equally spaced in all directions.

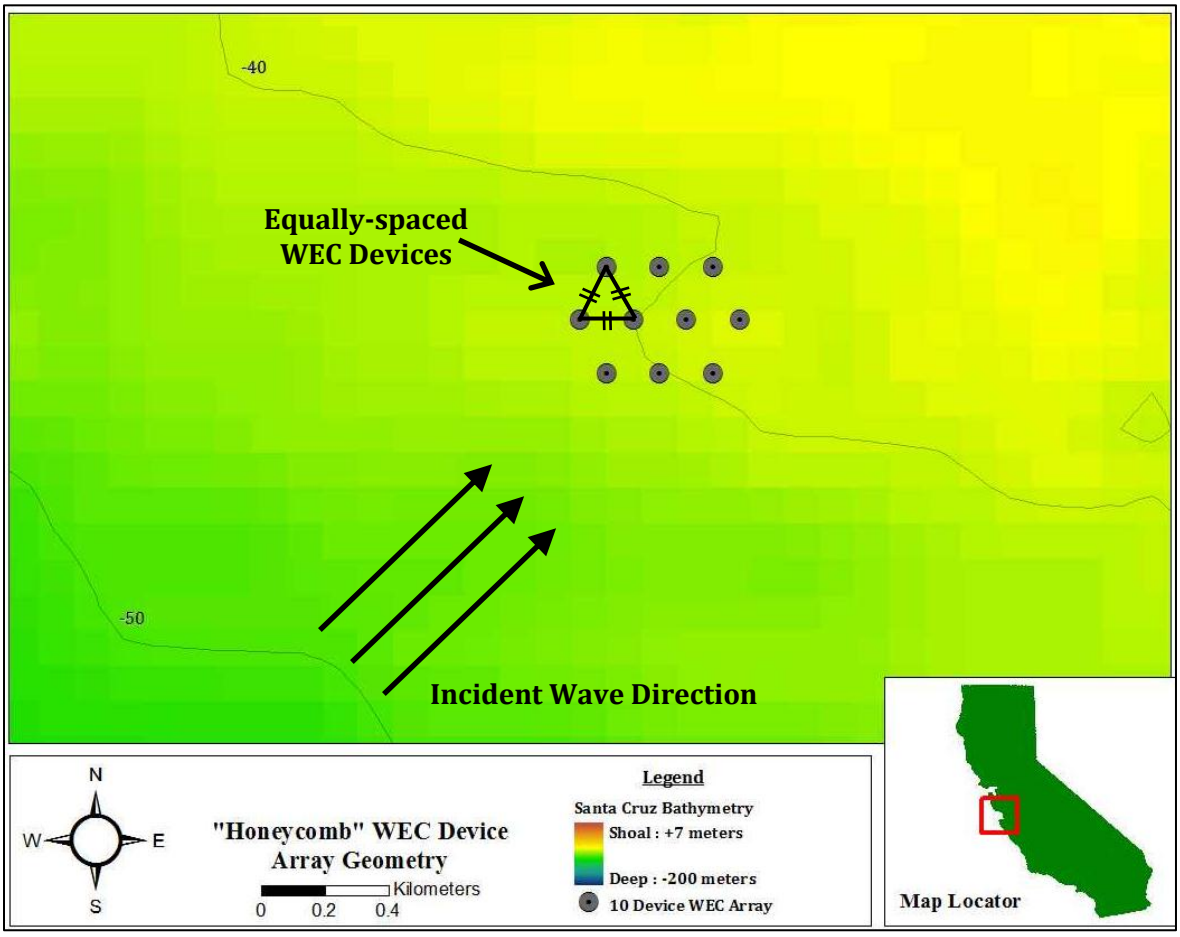

Figure 2. Example honeycomb geometry of a 10-WEC device array in the model. The 40 m and 50 m depth contours are shown for reference.

A previous sensitivity analysis of SWAN model parameters investigated the effects of specific SWAN model parameters on the wave properties in proximity to a WEC array (analysis summarized in Appendix B; full report in SNL, 2011):

- Wave energy transmission coefficient (fraction of wave energy allowed to pass an obstacle)
- Wave energy reflection coefficient (fraction of wave energy reflected from an obstacle)
- Frequency spreading coefficient (amount of spreading occurring in the frequency wave spectrum)
- Directional spreading coefficient (amount of spreading occurring in the directional wave spectrum).

From the previous sensitivity analysis, it was determined that the SWAN transmission coefficient had the largest effect on wave parameters when obstacles were simulated, and that varying the other parameters had negligible impacts in comparison.

Therefore, only the SWAN transmission coefficient was included in the present evaluation. In addition, variation in the number of WEC devices in an array and the array deployment location (depth contour) were investigated. In the present sensitivity analysis:

- The WEC array device numbers were varied between 10, 50, 100 and 200 WEC devices
- The arrays locations were centered on the 40 meter, 50 meter and 60 meter depth contours south of Santa Cruz, CA
- The wave energy transmission coefficient was varied between 0.3 and 0.7 (30% to 70% of incident wave energy allowed to pass each WEC device).

Model Boundary Conditions

Historical wave conditions offshore of Monterey Bay are fairly well understood due to the existence of long-term wave data measurements from several NOAA NDBC and CDIP buoys. For the present analysis, representative data from NOAA NDBC buoy #46042 were utilized to determine typical wave conditions to be expected in the Monterey Bay region. The buoy is located 27 nautical miles west-northwest of Monterey, CA, in greater than 2000 meters water depth. Data have been recorded at this location since 1987, making it a statistically reliable source for evaluating typical (and extreme) wave conditions approaching Monterey Bay.

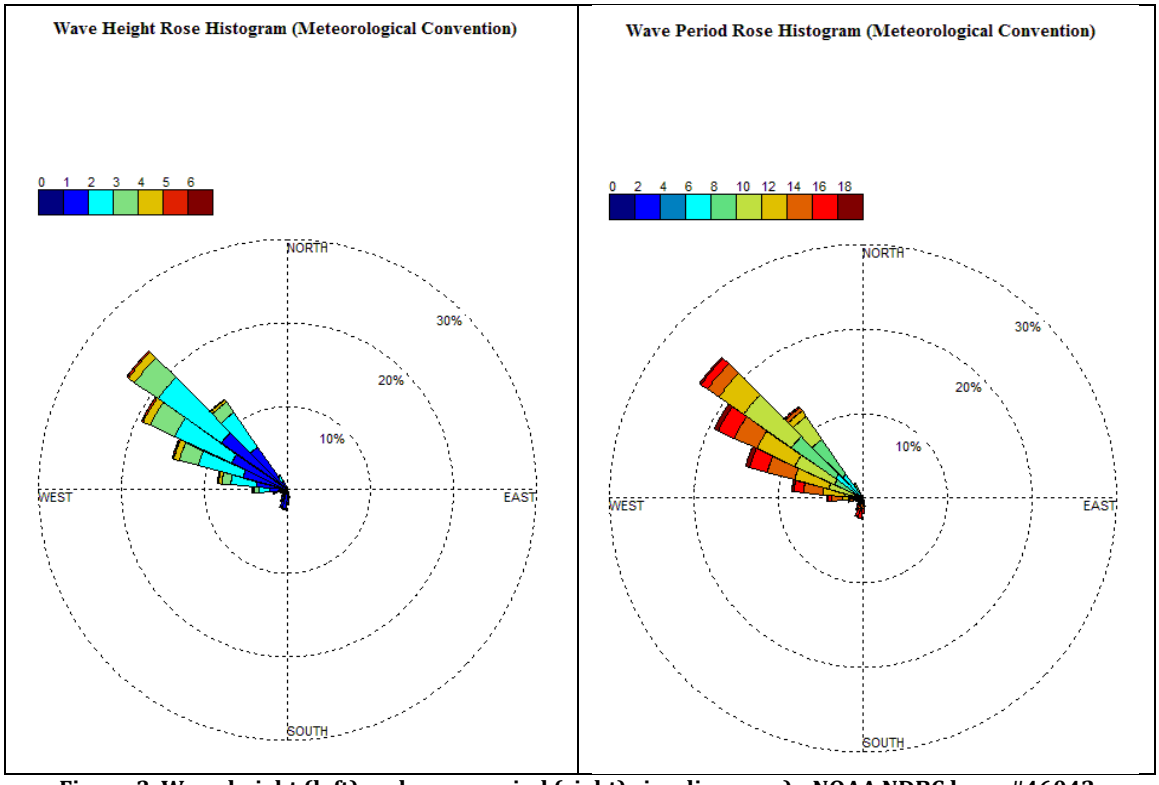

Figure 3. Wave height (left) and wave period (right) rise diagrams) - NOAA NDBC buoy #46042.
(Direction <u>from</u> which the waves are approaching)

A wave height and wave period rose was generated by the historical data to evaluate the historical wave climate.[1] Significant wave height is the average of the highest 1/3 of wave heights on record. Dominant wave periods correspond directly to the frequency containing the largest amount of wave energy. Mean wave directions are the directions *from* which the dominant waves (waves corresponding to the dominant period) are approaching.

Figure 3 illustrates that the dominant wave direction (most frequently occurring) was from the northwesterly direction. The plots also indicate the most frequently occurring wave heights and wave periods (magnitude of color bands in plots). The basic statistics (of all available wave data from this buoy) that resulted from the wave data analysis are listed in Table 1. Figure 4-Figure 6 show the statistical histograms of each wave property and provide a visual comparison to the model input values selected for the present modeling effort. It is evident that the majority of the waves approach the Monterey Bay region from the Northwest (270-360 degrees True North) and that more than half of the waves on record comprised of wave heights of 2.0 meters or less and wave periods of less than 12 seconds.

Table 1. Statistical data analysis - NOAA NDBC buoy #46042

	Mean Value	Median Value	Mode Value
Hs (m)	2.2	2.0	1.7
Tp (sec)	11.8	11.4	12.5
MWD (degrees)	287.5	299	310

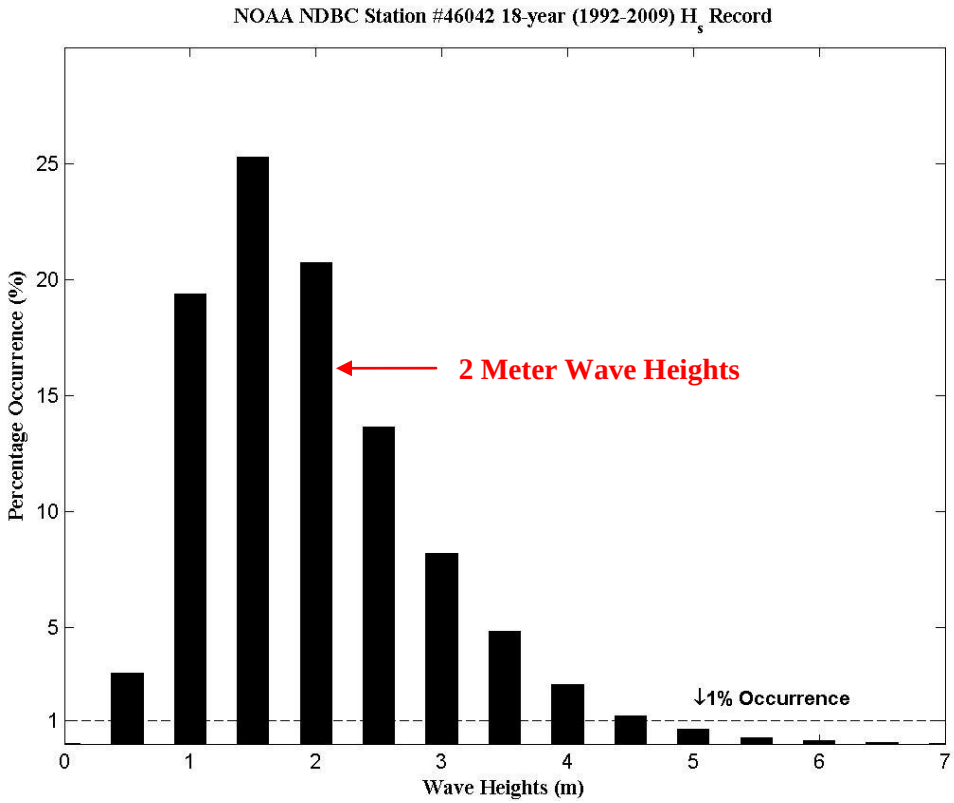

Figure 4. Wave height histogram (frequency of occurrence) - NOAA NDBC buoy #46042.

[1] Wave heights are the significant wave heights; the wave periods are the dominant wave periods. The wave directions are the mean wave direction, MWD, recorded by the buoy, and are the directions *from* which the waves approach.

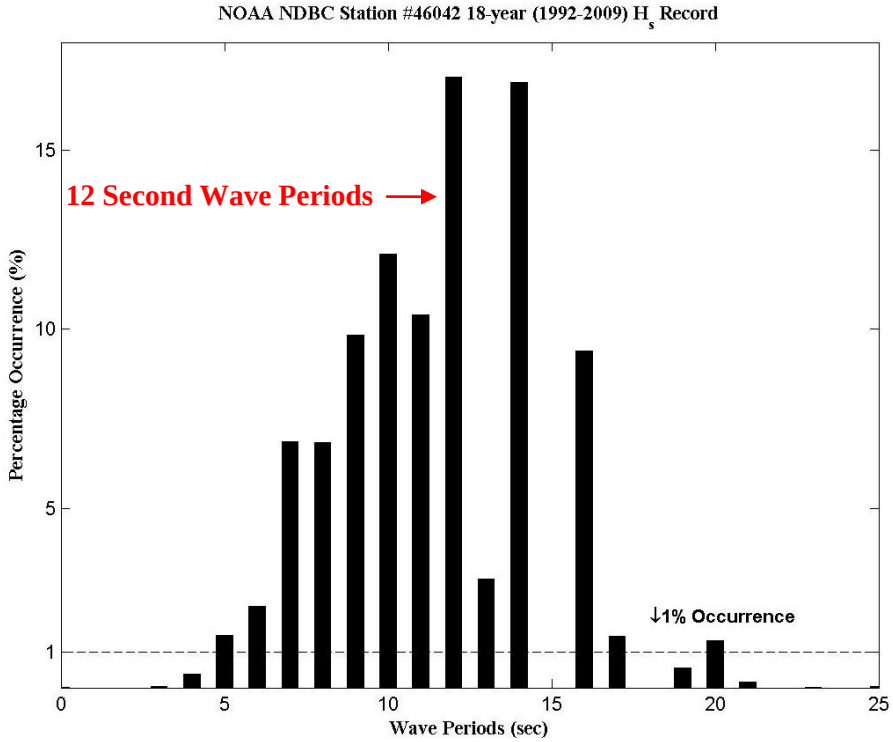

Figure 5. Wave period histogram (frequency of occurrence) - NOAA NDBC buoy #46042.

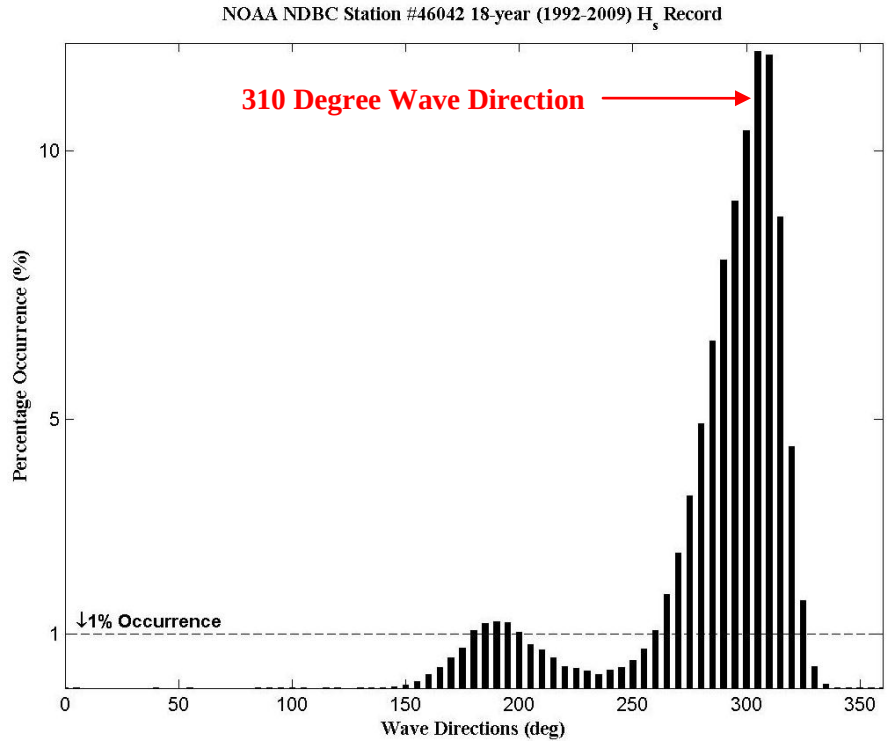

Figure 6. Wave direction histogram (frequency of occurrence) - NOAA NDBC buoy #46042.

The objective of the present investigation, however, is to evaluate the near- and far-field effects of WEC devices and arrays on the near-shore environment. Specifically, this will be accomplished by

assessing wave property changes in lee of WEC arrays, and the horizontal extent over which these changes are expected. To do so, the potential wave property changes in proximity to the nearest shoreline (e.g. Santa Cruz, CA) must be explored.

Due to the sheltered location of the City of Santa Cruz along the northern Monterey Bay shoreline, and the hypothetical placement of the WEC arrays immediately south of Santa Cruz, it is believed that waves approaching from the Northwest and/or West will have minor negative impacts on the wave and current climate at Santa Cruz beaches[2]. Even with wave refraction effects, the Northwesterly-incident waves at the 50 meter depth contour near Santa Cruz still approached the array from a westerly direction (SNL, 2011); and the shoreline to the east was of sufficient distance in lee (order 15 km) that the modeled wave energy spectrum near the eastern shoreline did not indicate evidence of altered wave properties (i.e. the wave energy spectrum had 'recovered' from the wave shadowing effects due to directional wave spreading).

In order to model a scenario with potential near-shore (and shoreline) Santa Cruz impacts, a representative offshore wave condition was selected for the present study that has the potential to alter near-shore wave properties. Based on the data analyzed from NOAA NDBC buoy #46042, the mode of the wave heights and periods, 1.7 m and 12.5 sec, respectively, was selected for representative offshore boundary conditions. The offshore mean wave direction applied at the boundaries was 205-degrees, chosen because it causes wave shadowing to occur in the direction of the nearest shoreline (order 5 km) to the WEC deployment locations (at Santa Cruz).

This is, admittedly, a conservative effort at modeling WEC array impacts on near-shore wave properties because waves approach Santa Cruz from a southwesterly direction (180°-270° True North) approximately 15% of the time. On the other hand, waves approach the region from a northwesterly direction (270°-360° True North) approximately 80% of the time. It will, however, illustrate the potential effects on wave properties near the Santa Cruz shoreline if a WEC array were to be installed in this location offshore of Santa Cruz.

Table 2 lists the offshore Monterey Bay model boundary conditions selected for the present sensitivity analysis.

Table 2. Model Boundary Conditions.

Parameter	Value
Hs (m)	1.7
Tp (sec)	12.5
MWD (degrees)	205

Model Domain

The Monterey Bay model domain is shown throughout Figure 1 above. The inner dashed outline denotes the nested Santa Cruz model domain. Offshore model boundary conditions were specified for all "wet" boundaries (north, west and south sides) of the Monterey Bay domain. Waves were propagated from offshore to onshore throughout the entire domain. Wave frequency and directional spectra were extracted along the "wet" boundaries of the Santa Cruz domain and used as input boundary conditions for the nested, Santa Cruz domain (Figure 7).

[2] This statement requires a comprehensive and thorough sensitivity analysis to validate; however, the referenced previous sensitivity analysis (SNL, 2011) indicated minor potential for negative effects along the Santa Cruz shoreline when waves approach from the Northwesterly directions.

Waves were then propagated from the offshore boundaries of the Santa Cruz model domain to the shoreline. A baseline condition was modeled in which no obstacles were incorporated (no WEC devices simulated) to "absorb" wave energy. Then, scenarios that included obstacles were modeled to ascertain the effects of the obstacles on the wave properties and the model sensitivity to varying wave energy transmission coefficient, WEC array size and WEC array deployment location (depth contour).

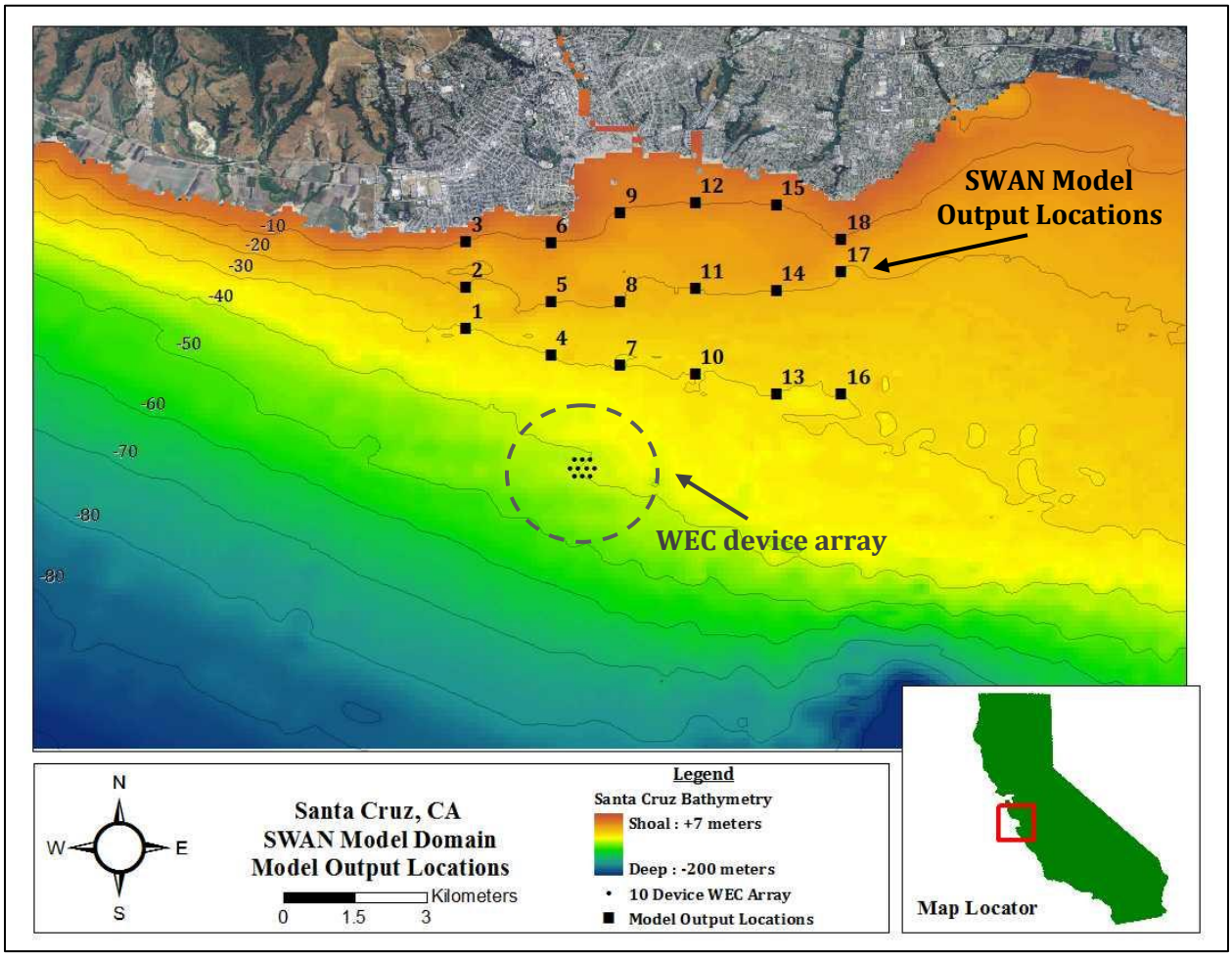

Figure 7. Nested Santa Cruz domain with example WEC device array (gray dashed circle) and model output locations (black squares) shown.

In order to evaluate the effects of the WEC array and associated model parameters on the wave propagation, output was extracted from 18 distinct locations during this evaluation (extraction point descriptions are listed in Table 3 and displayed in Figure 7). Six shoreline locations along the Santa Cruz coast were selected to span the anticipated horizontal extent of wave shadowing due to the WEC arrays (West to East):

- West Santa Cruz
- Steamer Lane
- Santa Cruz Wharf
- Santa Cruz Harbor
- East 26th Ave.
- Pleasure Point

Model output extraction occurred at three depth contours offshore of each shoreline location: the 30 m, 20m and 10 m depth contours, oriented and numbered sequentially south to north (see numbering in Figure 7).

These sections of the Santa Cruz shoreline are popular sight-seeing, surfing and recreation locations, with surf breaks, jogging paths and residential homes extending along the headlands and the beaches. Changes in near-shore wave conditions due to the WEC array, if any, are important to ascertain at this location since this will likely concern the recreational community. Furthermore, changes in wave conditions at these near-shore locations are important to evaluate from the perspective of tidal circulation, shoreline erosion, and ecological change.

Table 3. Model output location number, depth contour and descriptions.

Model Output Location	Depth Contour and Description	Model Output Location	Depth Contour and Description
1	30 m - West Santa Cruz	10	30 m – Santa Cruz Harbor
2	20 m - West Santa Cruz	11	20 m – Santa Cruz Harbor
3	10 m - West Santa Cruz	12	10 m – Santa Cruz Harbor
4	30 m - Steamer Lane	13	30 m – East 26th Ave
5	20 m - Steamer Lane	14	20 m – East 26th Ave
6	10 m - Steamer Lane	15	10 m – East 26th Ave
7	30 m – Santa Cruz Wharf	16	30 m - Pleasure Point
8	20 m – Santa Cruz Wharf	17	20 m - Pleasure Point
9	10 m – Santa Cruz Wharf	18	10 m - Pleasure Point

Model Sensitivity Parameters

Within SWAN, the transmission coefficient determines the fraction of wave energy that is transmitted past the obstacles. The filter is applied uniformly across all wave frequencies. While prototype WEC device power take-off (PTO) may be directly related to specific wave frequencies (i.e. WEC devices may be tuned to absorb more energy from specific frequencies), investigation of model sensitivity to frequency-dependent transmission coefficients was not an objective of the present study. By varying the transmission coefficient within the model about reasonable values, the effect of the WEC devices energy absorption can be quantified.

In addition, the number of WEC devices within an array and the deployment location (depth contour) of the array center were varied within the sensitivity analysis. Larger numbers of WEC devices within an array may “absorb” a larger amount of wave energy, resulting in a larger wave shadow in lee of the array (both in horizontal extent and in magnitude of wave decrease). Further, the WEC device array may have a more significant impact on shorelines in lee of WEC arrays depending upon the depth contour at which the array is centered (i.e. the proximity of the shoreline to the WEC array). The full impact will depend on the depth at which the array is located as well as the bathymetry in lee of the array (i.e. is the lee bathymetry mild- or steep-sloped; or is there a large degree of elevation relief in lee of the array at which the wave refractive effects may be altered?).

SWAN allows the user to select from two different methods of implementing obstacles: 1) a basic representation using a constant transmission coefficient and 2) a more complex representation of simulating the obstacle as a dam, whereby the transmission coefficient depends upon the incident wave conditions and the obstacle height. Both methods allow a reflection coefficient to also be

specified (to represent reflected wave energy). The latter method requires additional coefficient specifications based upon published methods of computing wave energy transmission across a structure and is not incorporated here.

For this study, the former method of defining the transmission coefficient was selected for simplicity of evaluating the model sensitivity. The transmission coefficient ranges used in the sensitivity analysis, and the other parameter variations, are listed in Table 4. Table A.1 (Appendix A) lists the total number of runs and the parameter values corresponding to each run. For each scenario one transmission coefficient, one WEC array deployment location (depth contour), and one array size (number of devices) was selected. For brevity, Figure 8 simply shows an example of a 10-WEC array centered on three depth contours: 40 m, 50 m, and 60 m. Figure 9Figure 12 illustrate the 10-, 50-, 100- and 200-WEC arrays centered on the 40 m contour. These are the sample model setups for each of the respective wave modeling scenarios.

Table 4. Sensitivity analysis parameter values.

Parameter	Values
Transmission Coefficient (Fraction of Wave Energy Allowed to Pass)	[0.3, 0.4, 0.5, 0.6, 0.7]
WEC Location (Depth Contours)	[40 m, 50 m, 60 m]
WEC Array Size (# Devices)	[10, 50, 100, 200]

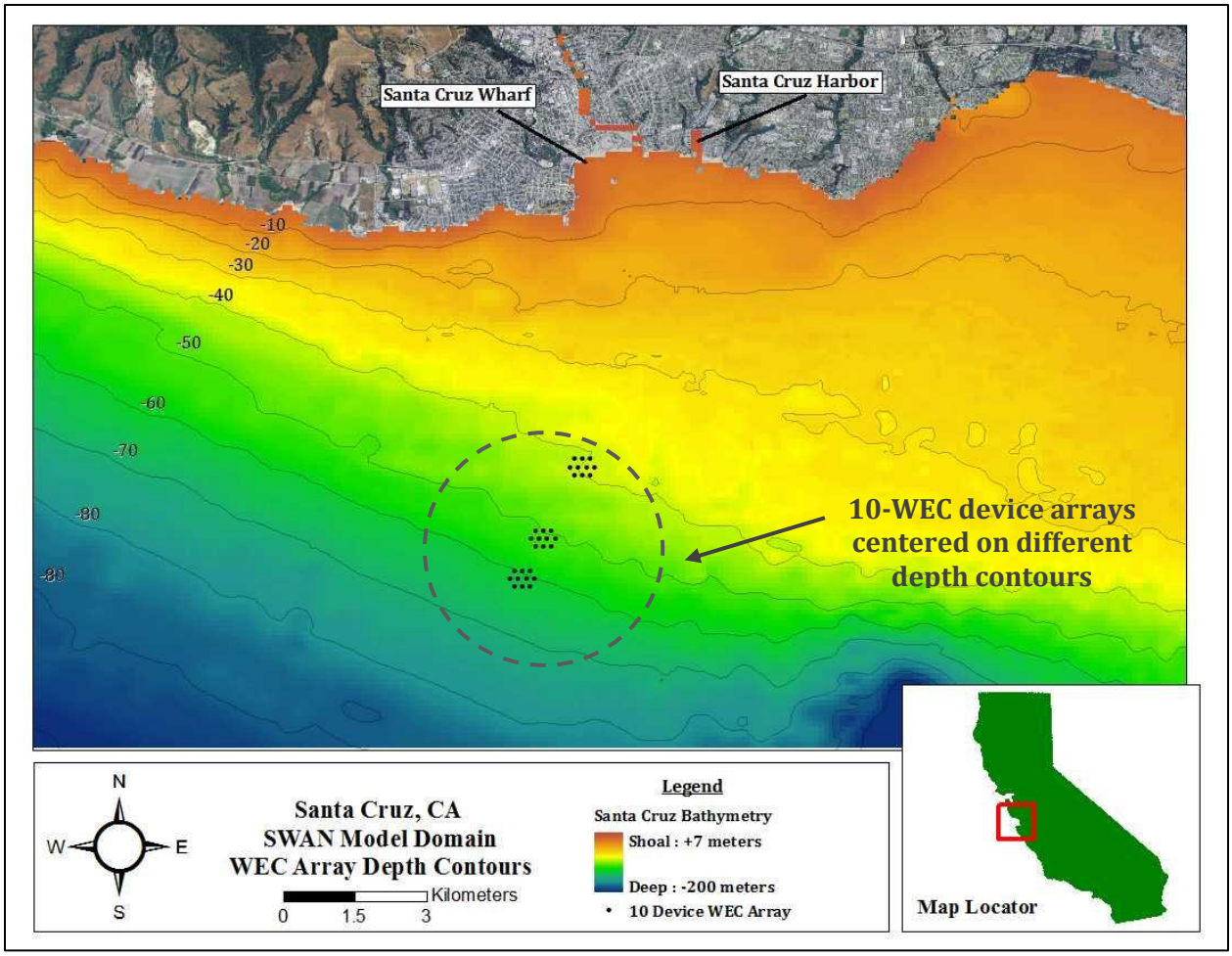

Figure 8. 10-WEC device arrays are shown centered on three different depth contours: 40 m, 50 m and 60 m.

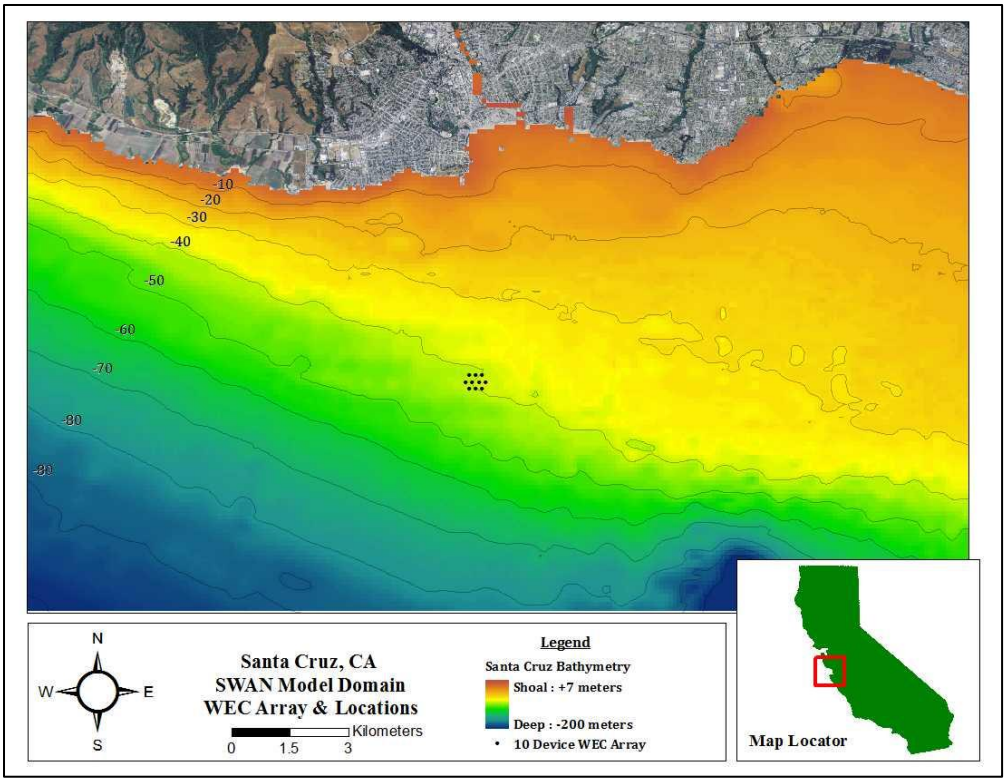

Figure 9. 10-WEC array centered on the 40 m depth contour.

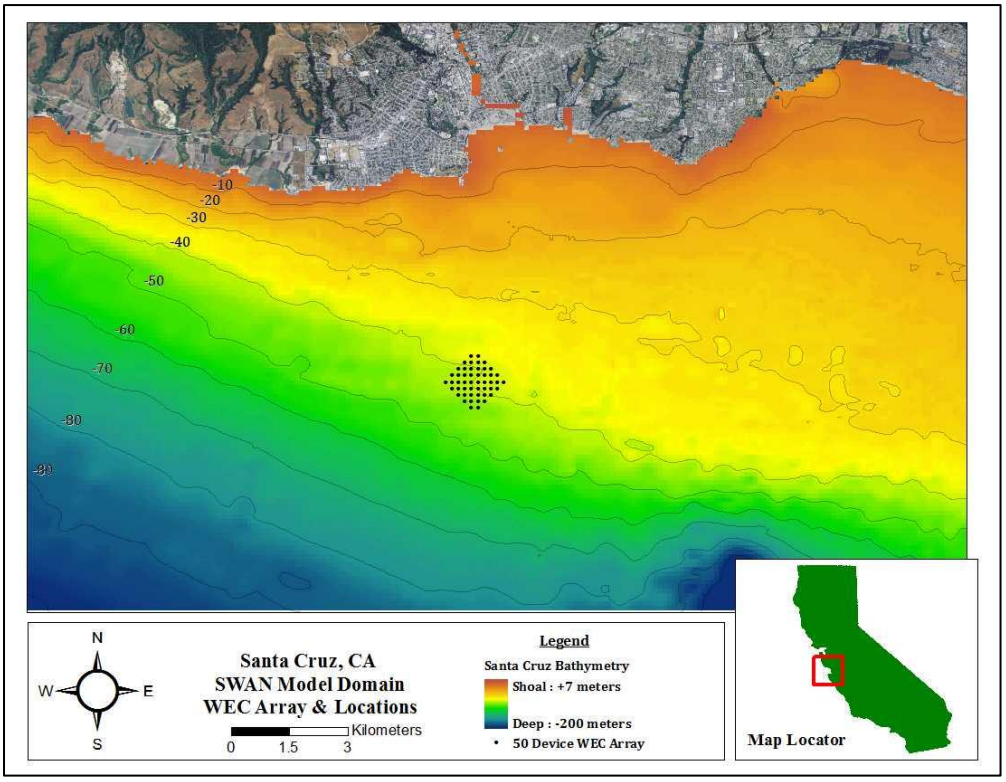

Figure 10. 50-WEC array centered on the 40 m depth contour.

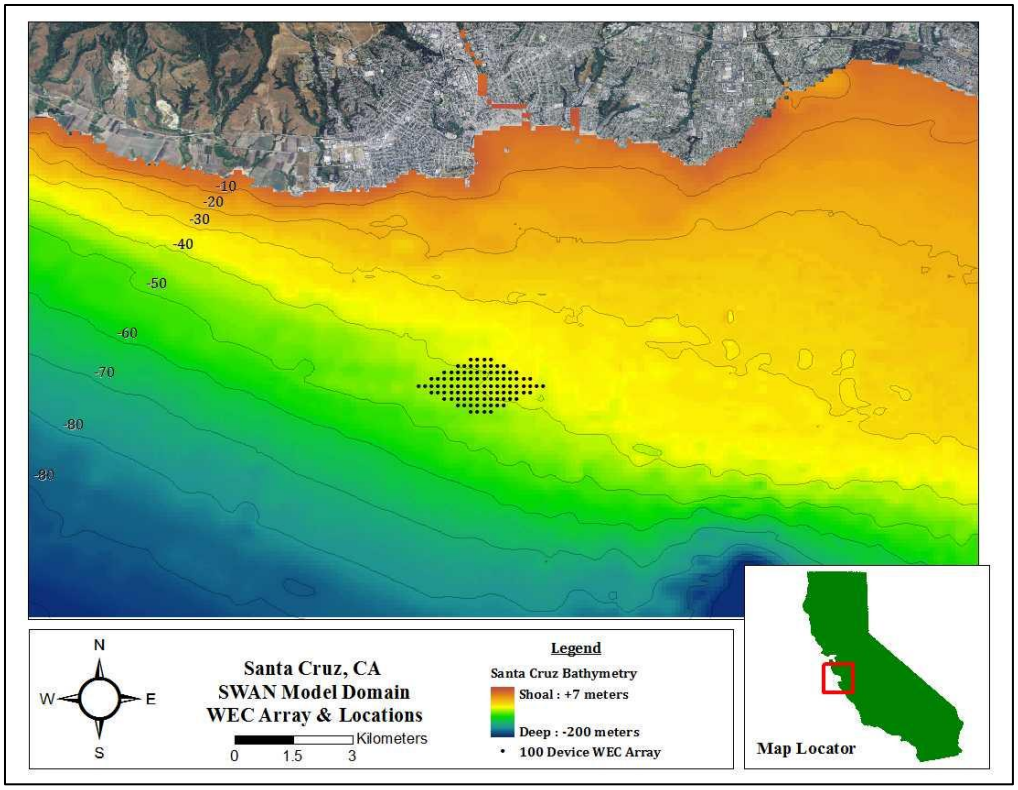

Figure 11. 100-WEC array centered on the 40 m depth contour.

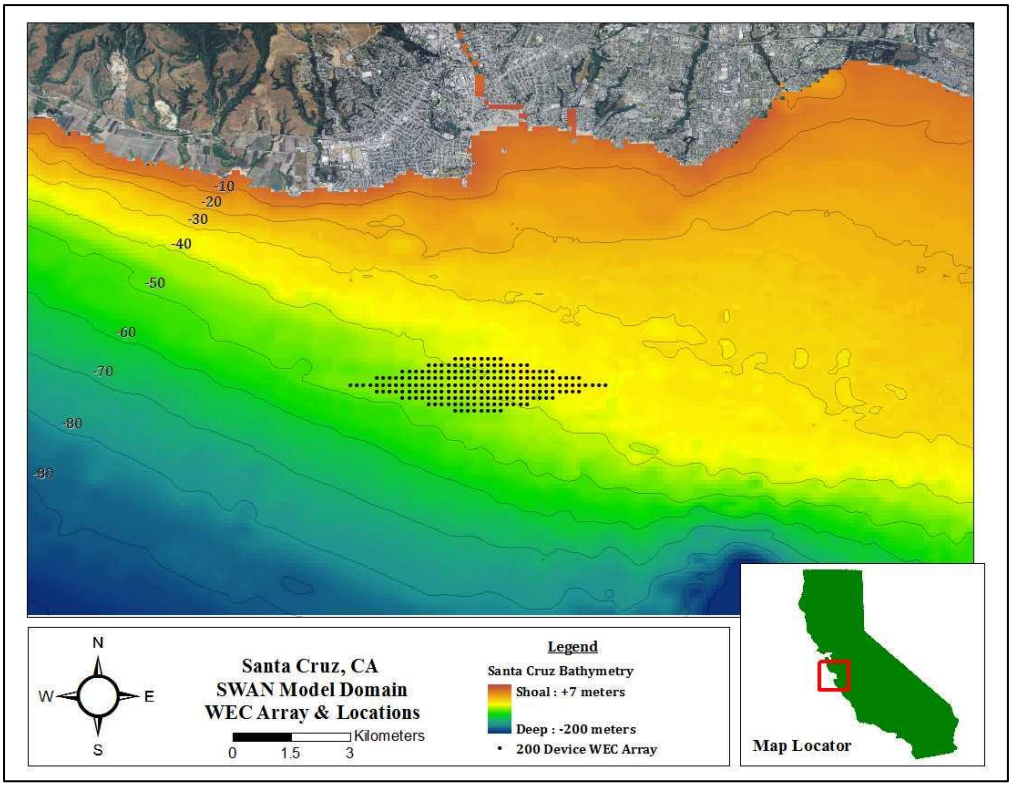

Figure 12. 200-WEC array centered on the 40 m depth contour.

Results and Discussion

Effects on Significant Wave Height

Model results were retained for each model run listed in Table A.1 (60 runs in total). Results included propagated wave heights, wave periods, wave directions, and near-bottom orbital velocities at all grid points in the model domains. Further, the same wave properties were extracted at each of the 18 distinct model output locations to facilitate simple point-to-point comparison.

Figure 13-Figure 15 show the results of significant wave height predictions from the sensitivity analysis. Images are surface-to-surface comparisons, comparing the modeled scenario results to the baseline scenario results. Black coloring indicates no (or negligible) change in wave height from the baseline scenario. Hotter colors indicate a larger amount of change (i.e. decrease in wave height) from the baseline scenario. Change is illustrated as a percentage change from the baseline scenario, computed as:

$$Percentage\ Change = \frac{(Initial\ Value - Final\ Value)}{Initial\ Value} \times 100$$

In addition, the percentage change computed at each of the 18 model output locations is listed as text in each sub-figure, adjacent to the output location number; this allows for rapid comparison of the effect on significant wave heights from case to case.

To illustrate a representative case in these figures, when not being varied the transmission coefficient is held constant at 0.5, the number of WEC devices held constant at 50, and the WEC device array location held constant at the 50 m depth contour.

Immediately evident from examination of these figures is that the largest wave height decreases in lee of the WEC arrays occur when the energy transmission is minimized (transmission coefficient is 0.3) and the number of WEC devices in an array is largest (e.g. 200 devices). Placement of the WEC array on the 40 m depth contour causes the largest near-shore wave height decreases along the Santa Cruz shoreline when compared to the 50 m or 60 m depth contour scenarios; however, it can be argued that placement at the 60 m depth contour, and, moreover, inclusion of a 200 WEC array, has the potential to disrupt a wider horizontal extent of significant wave heights (especially to the east of Santa Cruz, further east of the model output locations). Therefore, determination of a particular variable as the most sensitive variable in determining significant wave heights is difficult.

Effects on Near-bottom Orbital Velocities

Near-bottom orbital velocities (e.g. wave-driven currents) are directly proportional to the surface wave expression (i.e. significant wave height). Decreased wave heights cause a decrease in near-bottom orbital velocities, potentially altering the ambient wave-driven currents in a near-shore environment. Consequently, the percentage differences of the near-bottom orbital velocities are essentially equivalent to those computed from the significant wave height model scenarios. Figures of near-bottom orbital velocity percentage differences are not included since they are equivalent to Figure 13-Figure 15.

Effects on Peak Wave Periods

The percentage changes in peak wave periods during this study were negligible, as shown in Figure 16-Figure 18. The reason for this is twofold. First, within the model parameters, the frequency bin resolution may be too large to register small changes in wave periods (small changes in frequency

would not cause a change in frequency bin in model space). Second, since the model obstacles are "absorbing" the same percentage of wave energy from all wave frequencies (i.e. because the transmission coefficient is frequency-independent), there will be no change in peak wave energy; the dominant wave energy will not shift to an alternate frequency(ies). Therefore, in the present study, no change (or negligible change) will be observed.

Effects on Mean Wave Directions

Changes in mean wave directions are illustrated in Figure 19-Figure 21 as degrees changed (as opposed to percentage changes) for easy interpretation. Negative changes (blue) indicate clockwise (CW) rotation of wave direction. Positive changes (red) indicate counter-clockwise (CCW) rotation. Rotation, when it occurs, is relatively large, for the same reasons described for peak periods: the directional bin spacing was 15-degrees. Any changes less than this are indeterminable by the model.

Evident from the figures is that the mean wave directions are most affected by the largest WEC device array(s), which cause the largest horizontal extent wave shadowing effects in lee of the array(s). As a result of transmission coefficient and depth contour variation, mean wave directions are altered, but changes are minor.

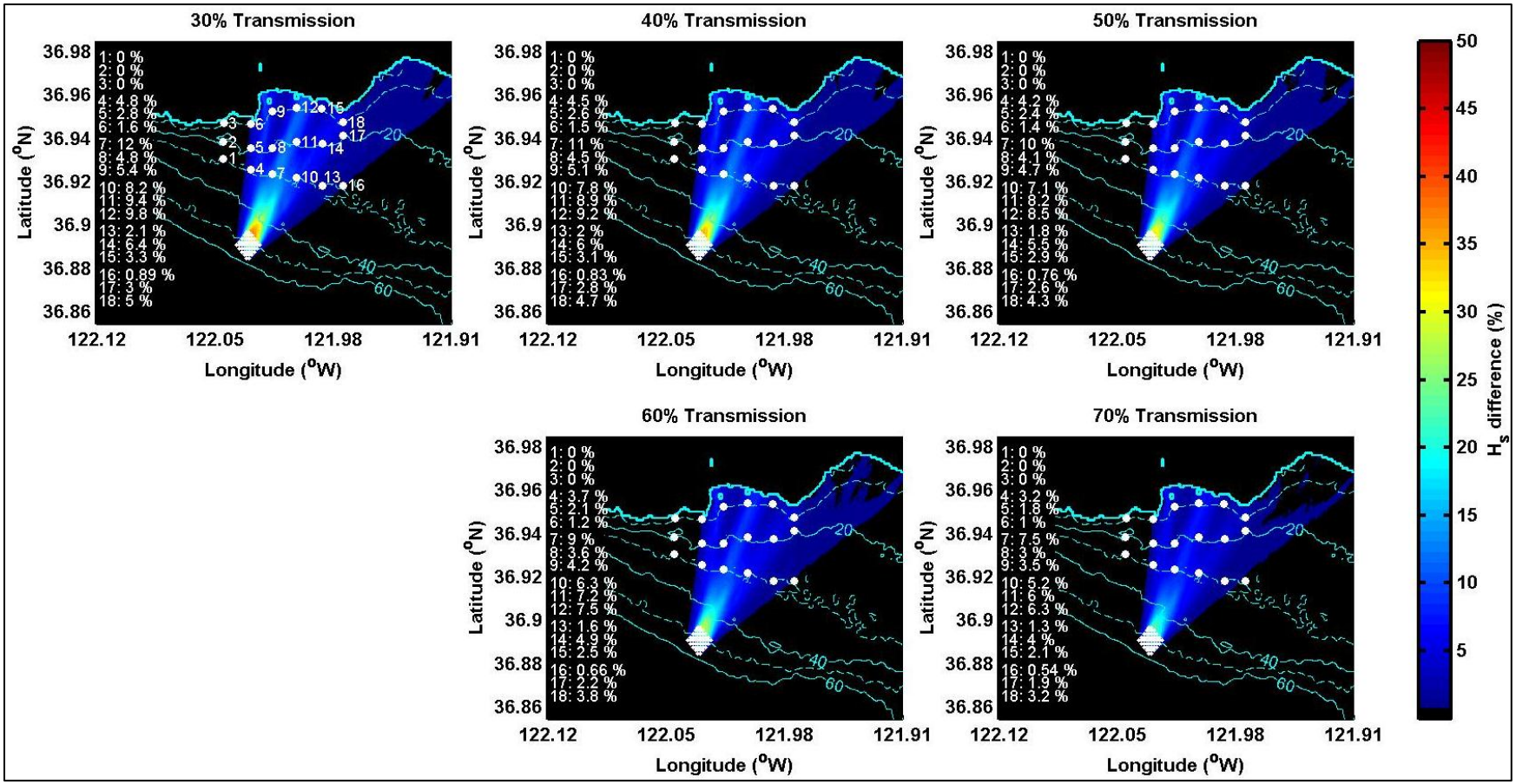

Figure 13. Significant wave height percentage decrease as a result of varying transmission coefficient. The WEC device array was centered on the 50 m depth contour and comprised 50 devices for all images below.

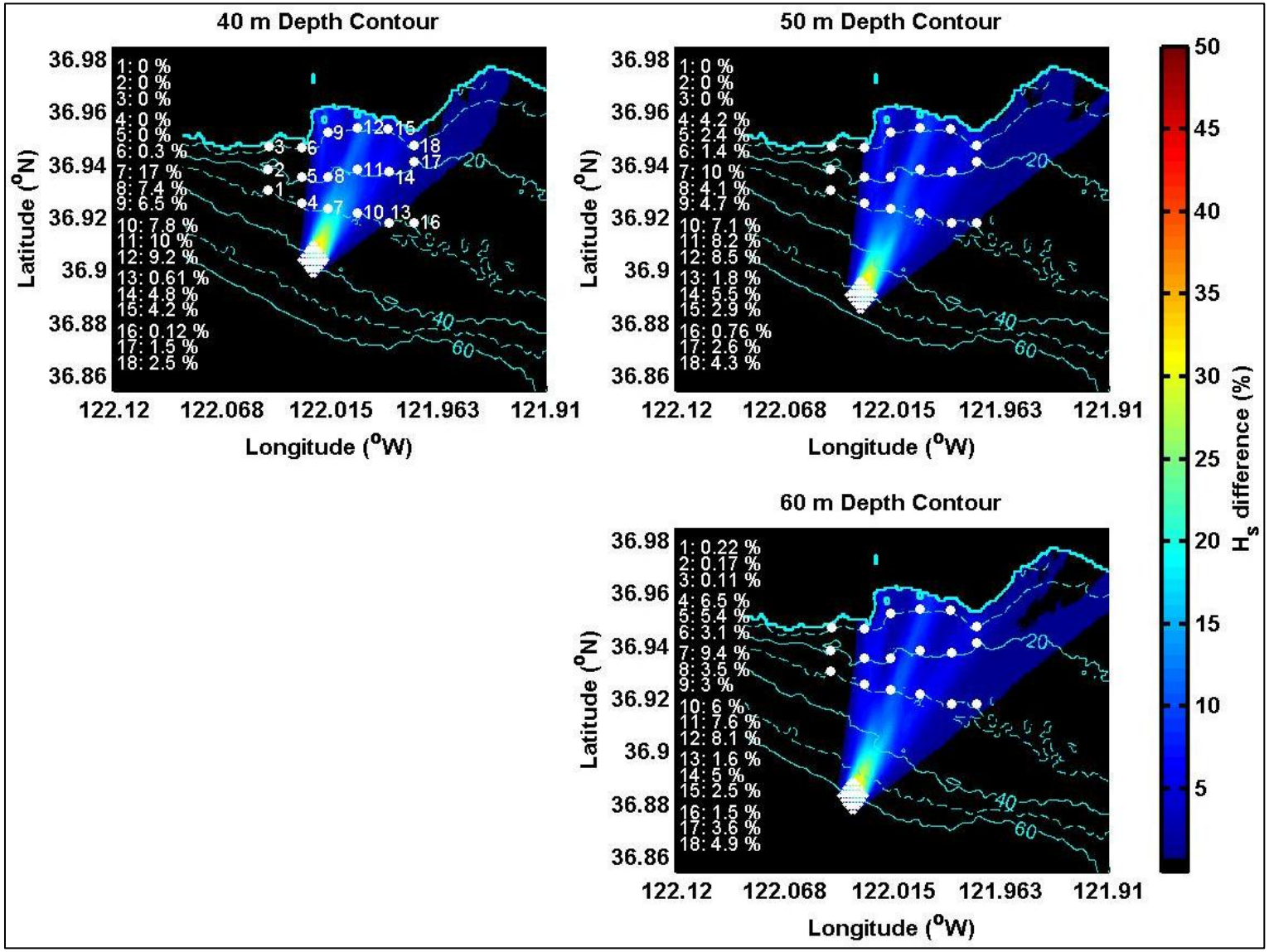

Figure 14. Significant wave height percentage decrease as a result of varying depth contour location.

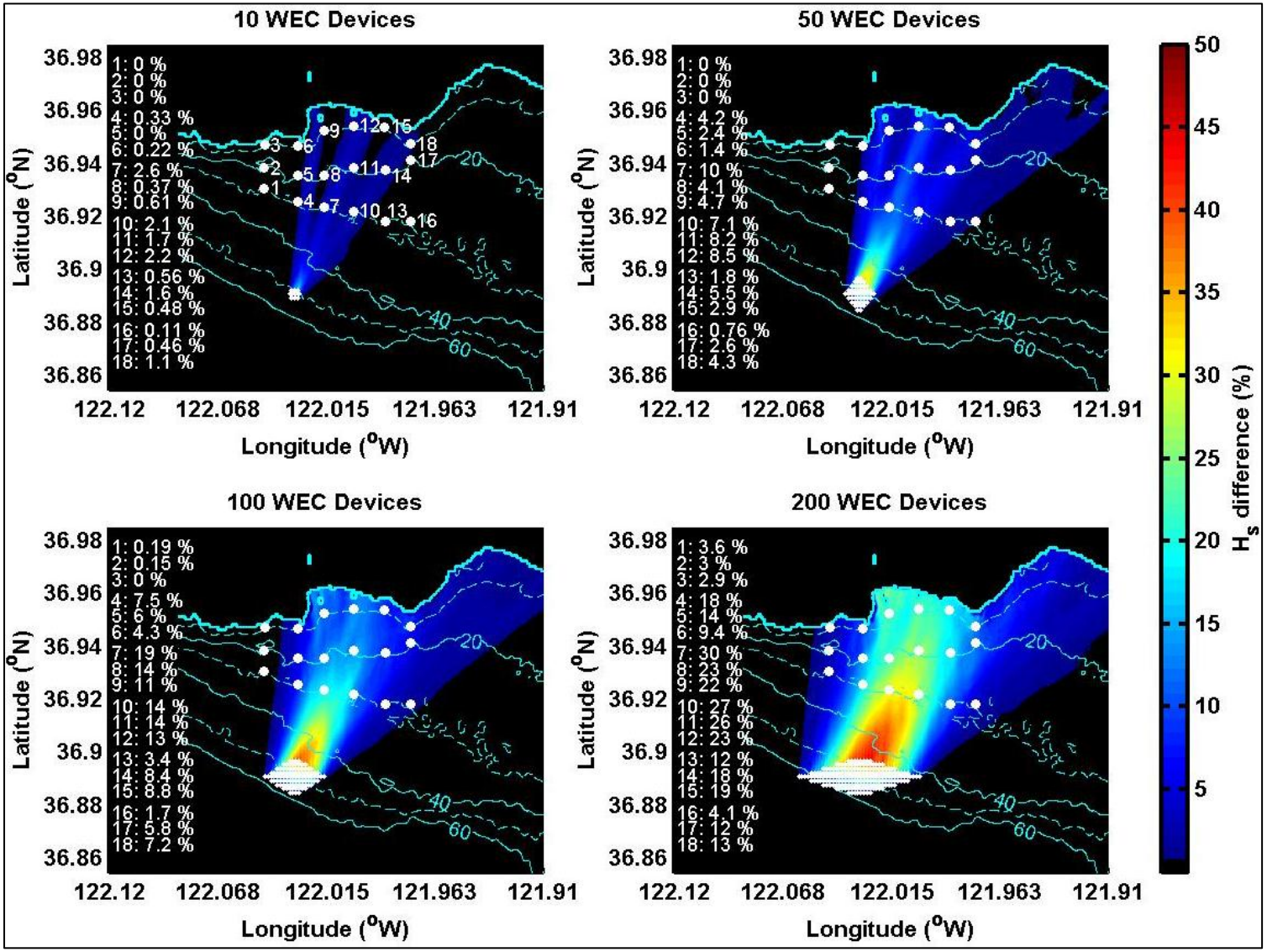

Figure 15. Significant wave height percentage decrease as a result of varying number of WEC devices in the array.

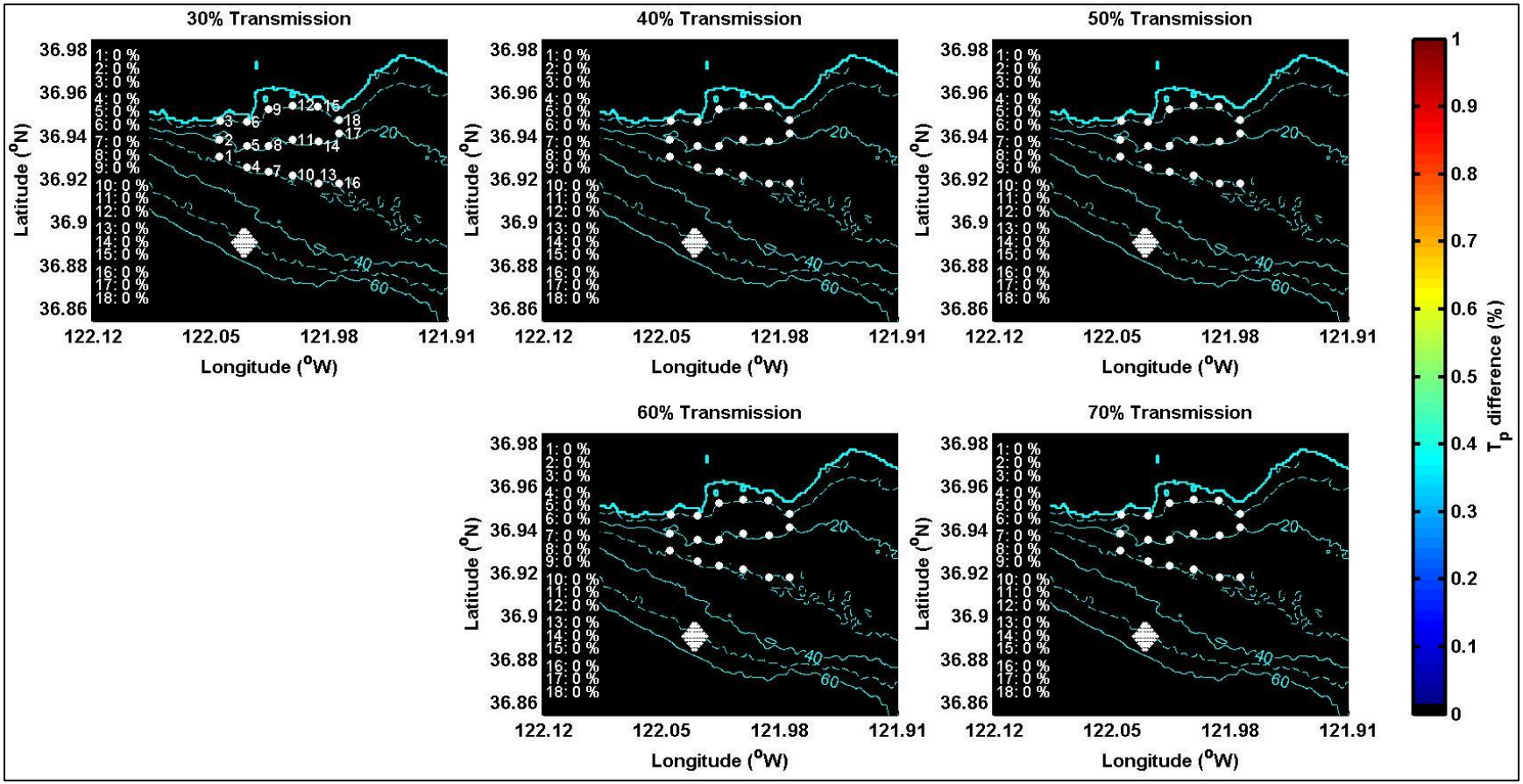

Figure 16. Peak wave period percentage decrease as a result of varying transmission coefficient.

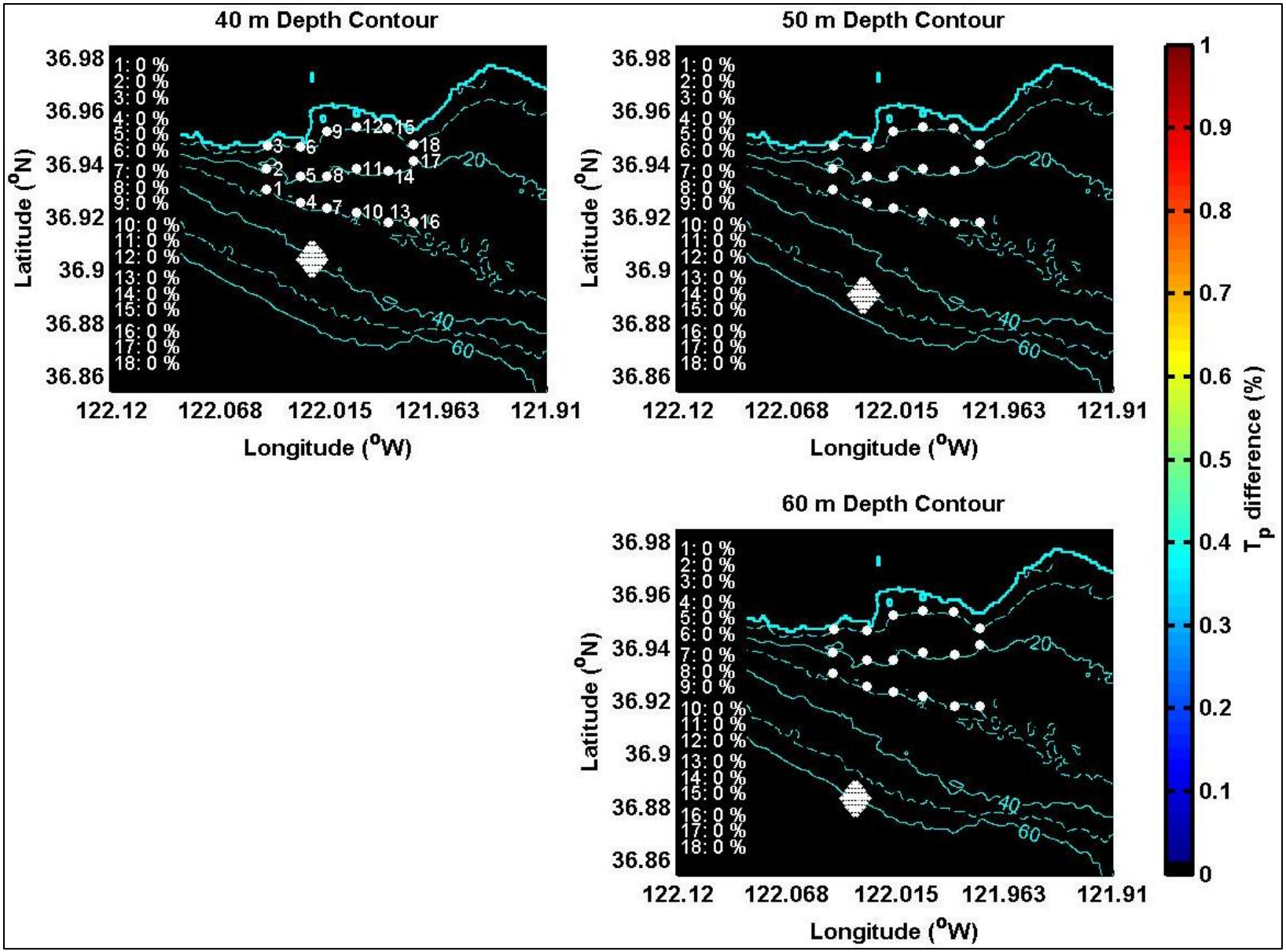

Figure 17. Peak wave period percentage decrease as a result of varying depth contour location.

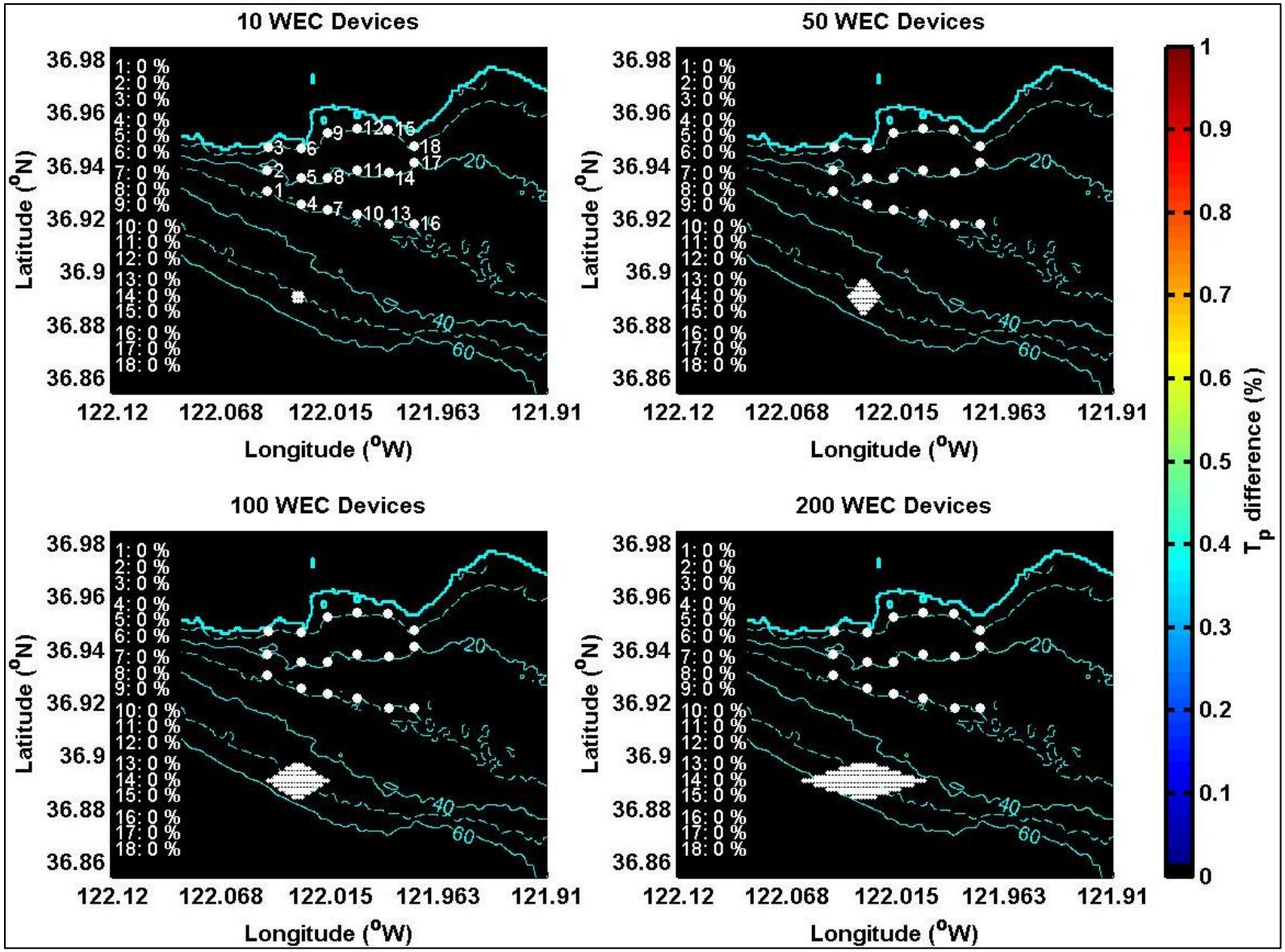

Figure 18. Peak wave period percentage decrease as a result of varying number of WEC devices in the array.

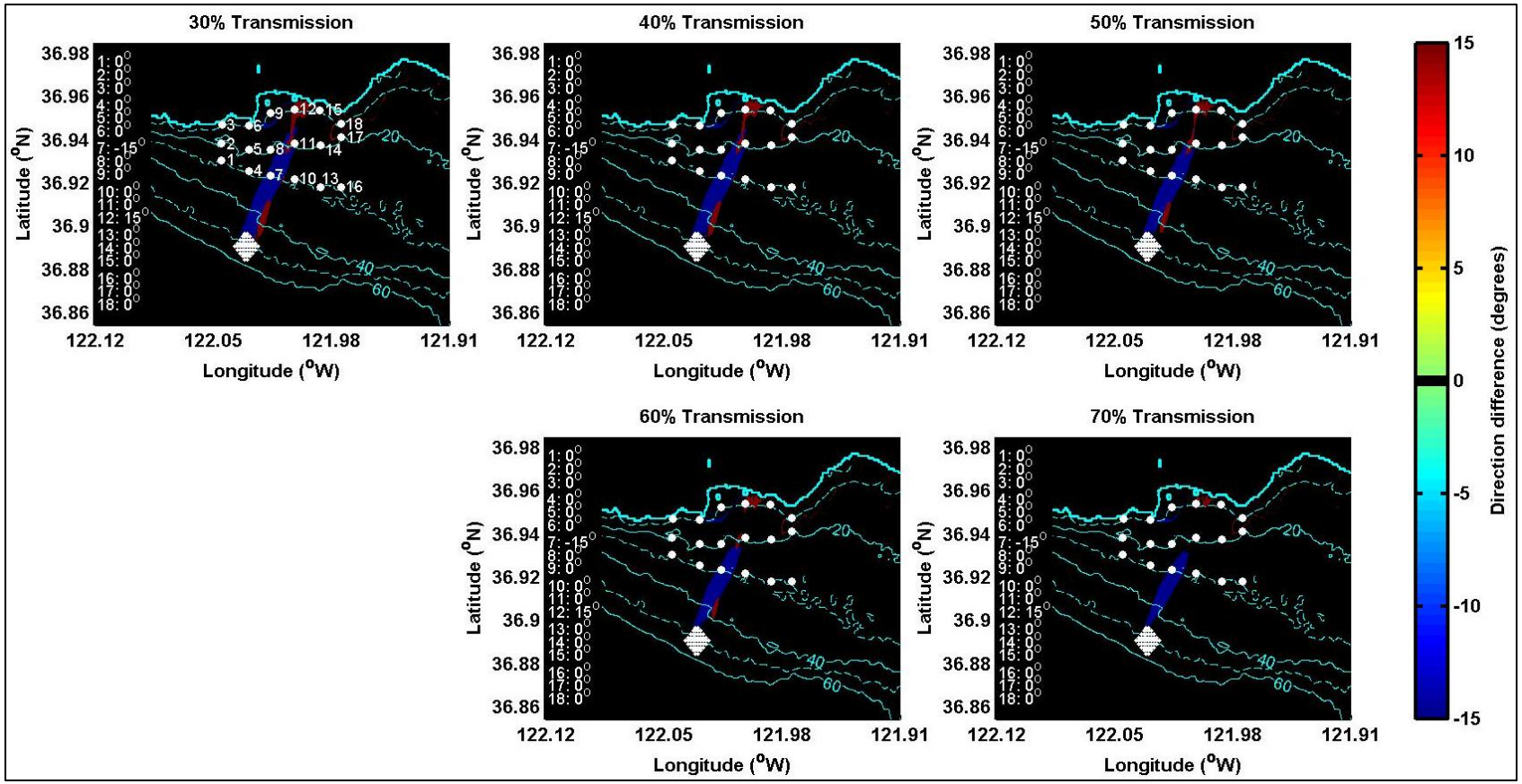

Figure 19. Mean wave direction change (degrees) as a result of varying transmission coefficient.

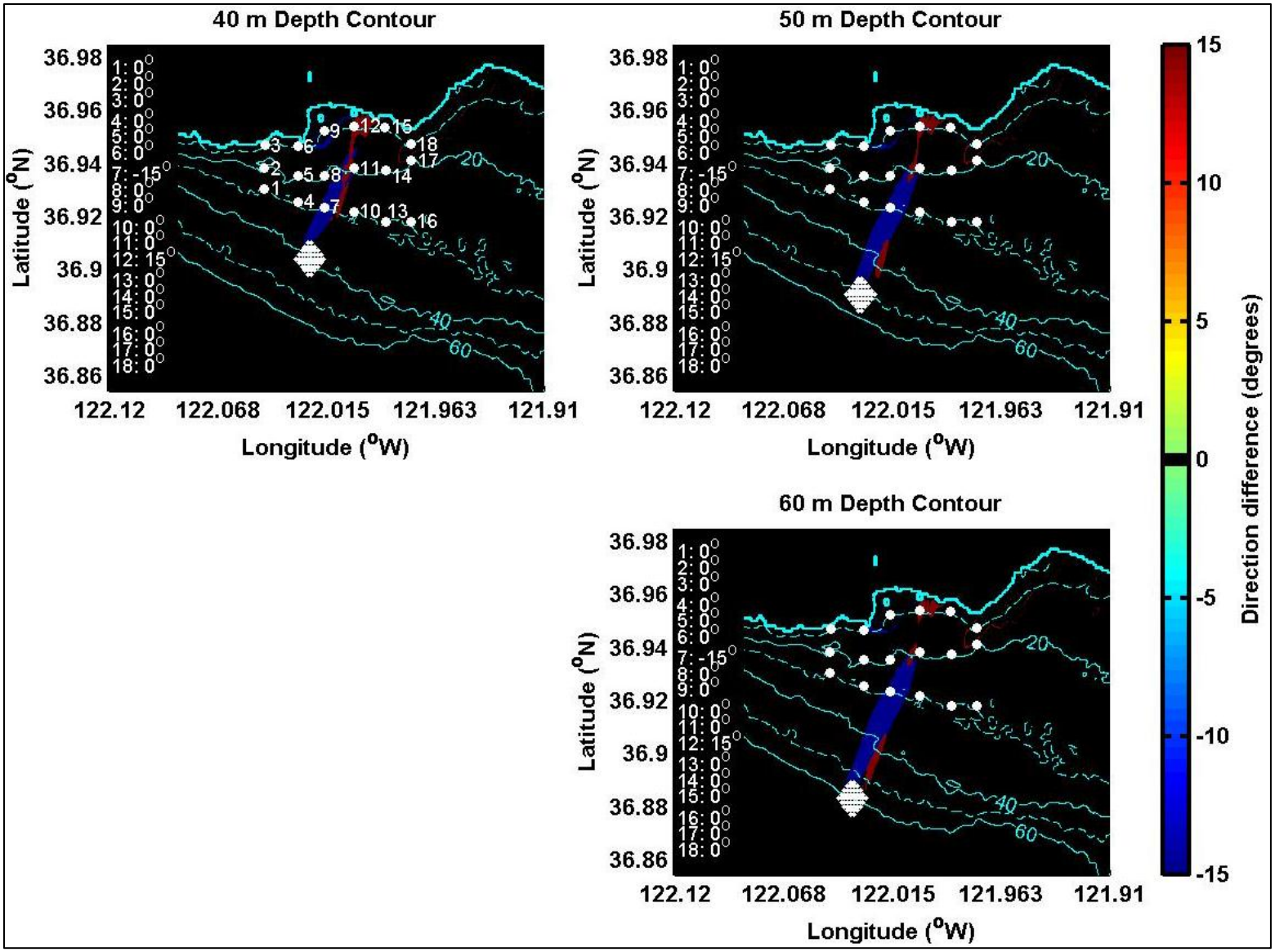

Figure 20. Mean wave direction change (degrees) as a result of varying depth contour location.

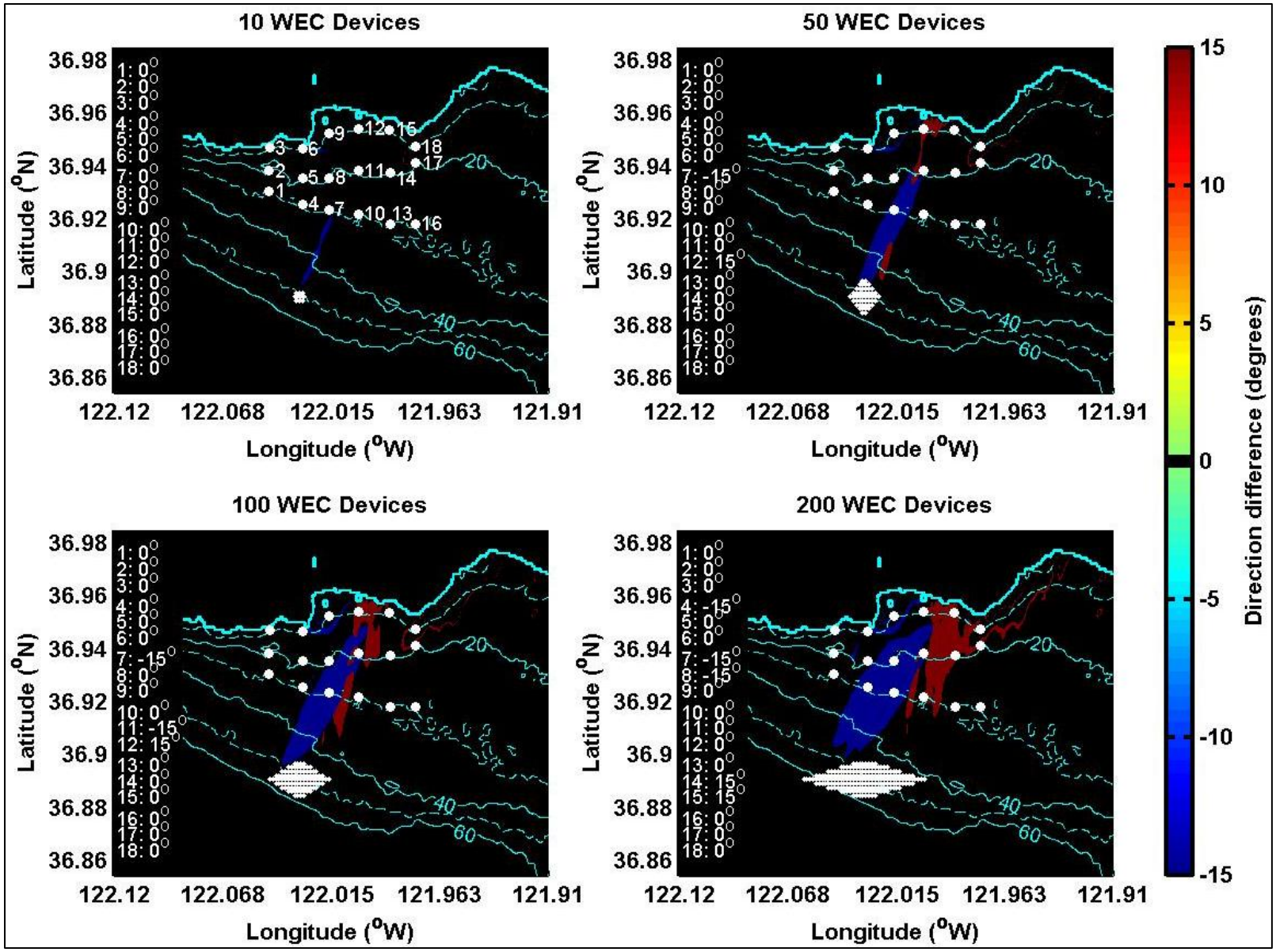

Figure 21. Mean wave direction change (degrees) as a result of varying number of WEC devices in the array.

Results Summary

Figure 22 illustrates the total variation in all wave conditions versus transmission coefficient for all scenarios modeled in the present study. The shape of the scatter plots and degree of vertical spreading that exists for each constant parameter are indications of the model sensitivity to that parameter. For example, setting the transmission coefficient to 0.3 and allowing all other sensitivity parameters to vary results in a minimum wave height decrease of 0% (no change) and a maximum decrease in wave height of ~42% over all scenarios modeled (top left subplot, Figure 22).

This figure illustrates that both wave height and near-bottom orbital velocity are subject to the largest potential variations, each decreasing in sensitivity as transmission coefficient increases. Wave direction is affected consistently for all transmission coefficients; and wave period is not affected (or negligibly affected) by varying transmission coefficient. Similar results are observed in Figure 23 and Figure 24, which indicate the range of changes anticipated by holding the depth contour and number of WEC devices in the array constant, respectively. Wave heights and near-bottom orbital velocities show the greatest amount of variation nearer to shore (40 m depth contour) and as the number of WEC devices in the array increases (200 device array).

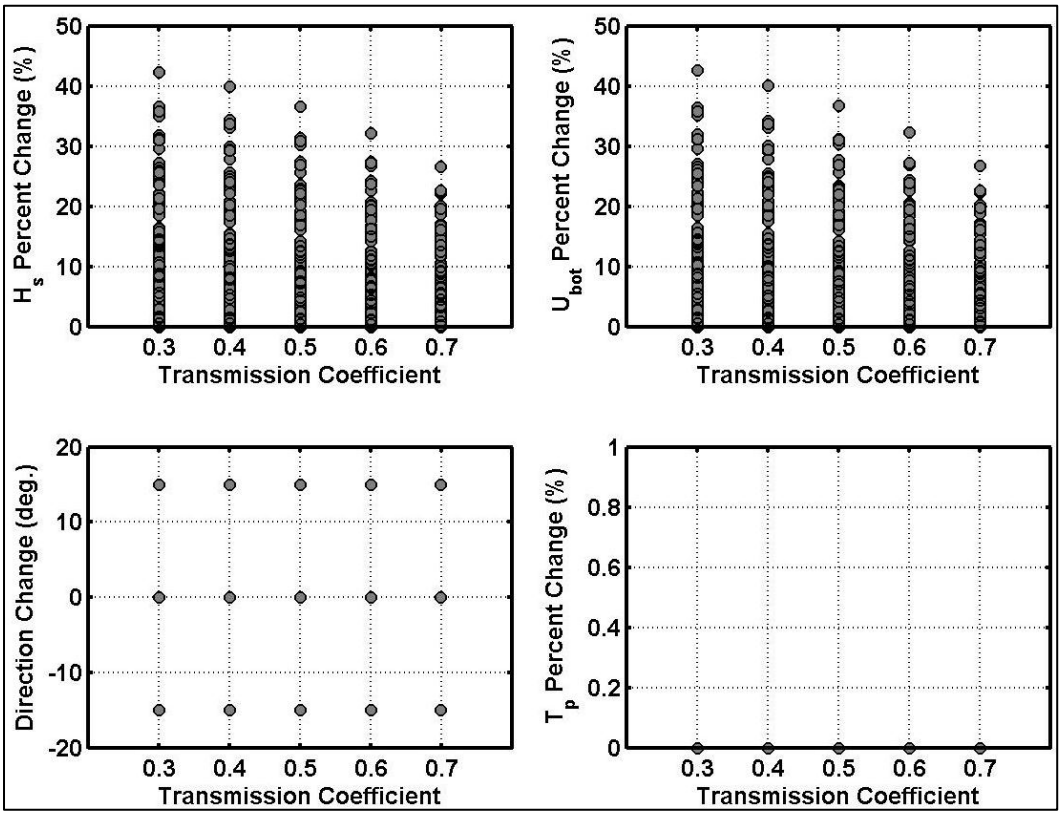

Figure 22. Variation in wave properties versus transmission coefficients.

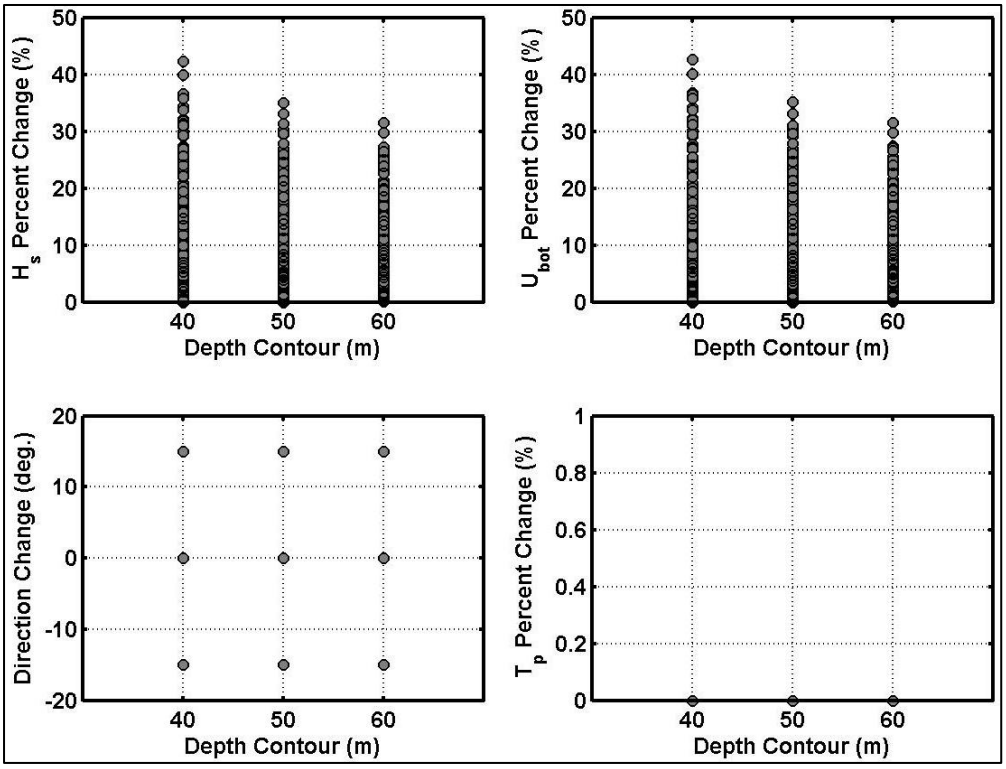

Figure 23. Variation in wave properties versus depth contours.

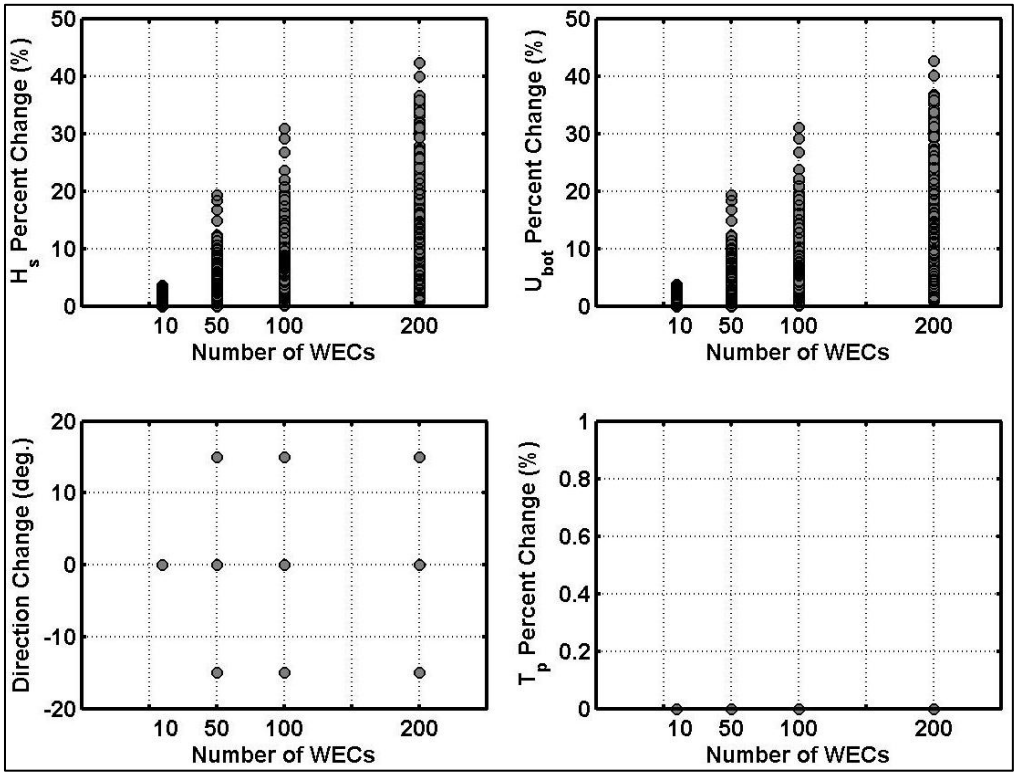

Figure 24. Variation in wave properties versus number of WEC devices in the array.

Another means of viewing the model results is presented in Figure 25 through Figure 27, which allow determination of the model parameters which have the greatest effect on the specific wave properties. From Figure 25 it is evident that the largest wave height variation is expected when the transmission coefficient is lowest (0.3), the deployment location is the shallowest (40 m depth contour), and the number of WEC devices in the array is the largest (200 devices). This scenario corresponds to the most wave energy "absorption", shallowest array location and largest horizontal extent "disruption" of wave energy propagation (due to the large number of obstacles).

The peak wave periods are not affected (or are negligibly affected) by variation of the parameters (Figure 26). The mean wave direction variation is minimized for the smallest number of WEC devices in the array (10 WEC devices, top left subplot); but remains constant for all other parameter variations (Figure 27).

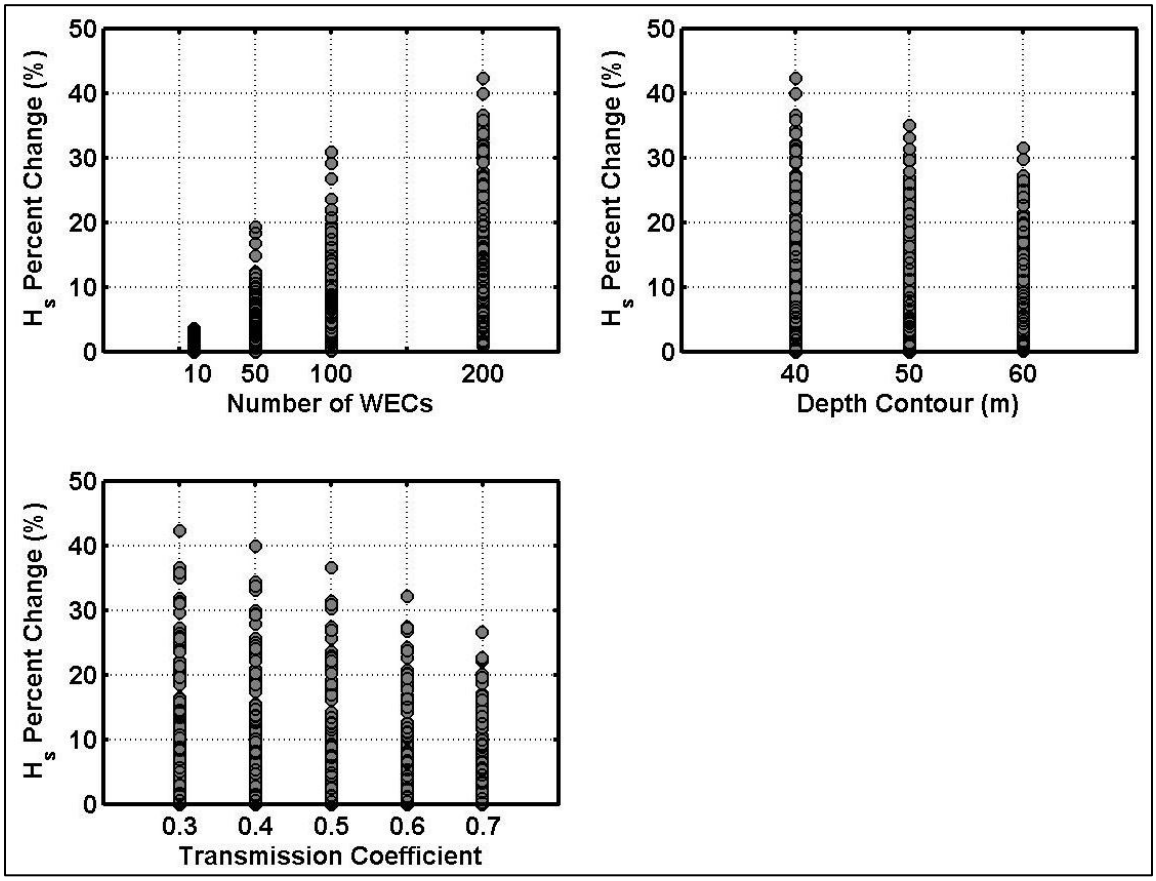

Figure 25. Variation in significant wave height for all varied parameters.

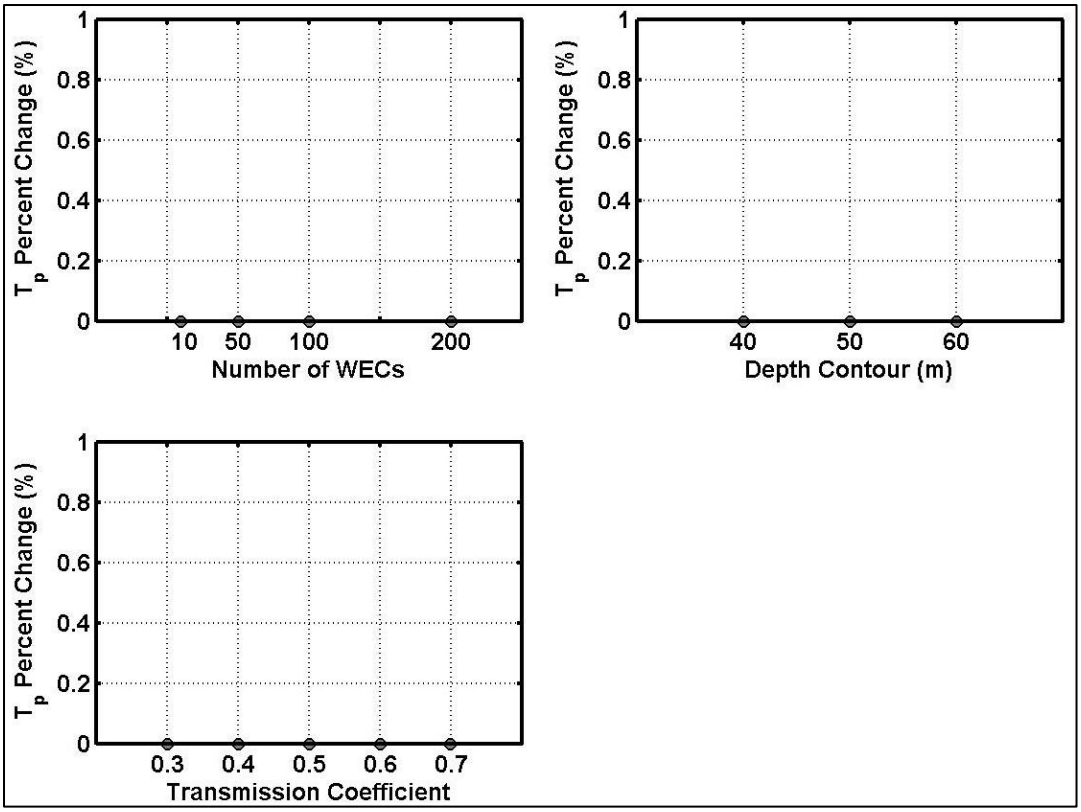

Figure 26. Variation in peak wave period for all varied parameters.

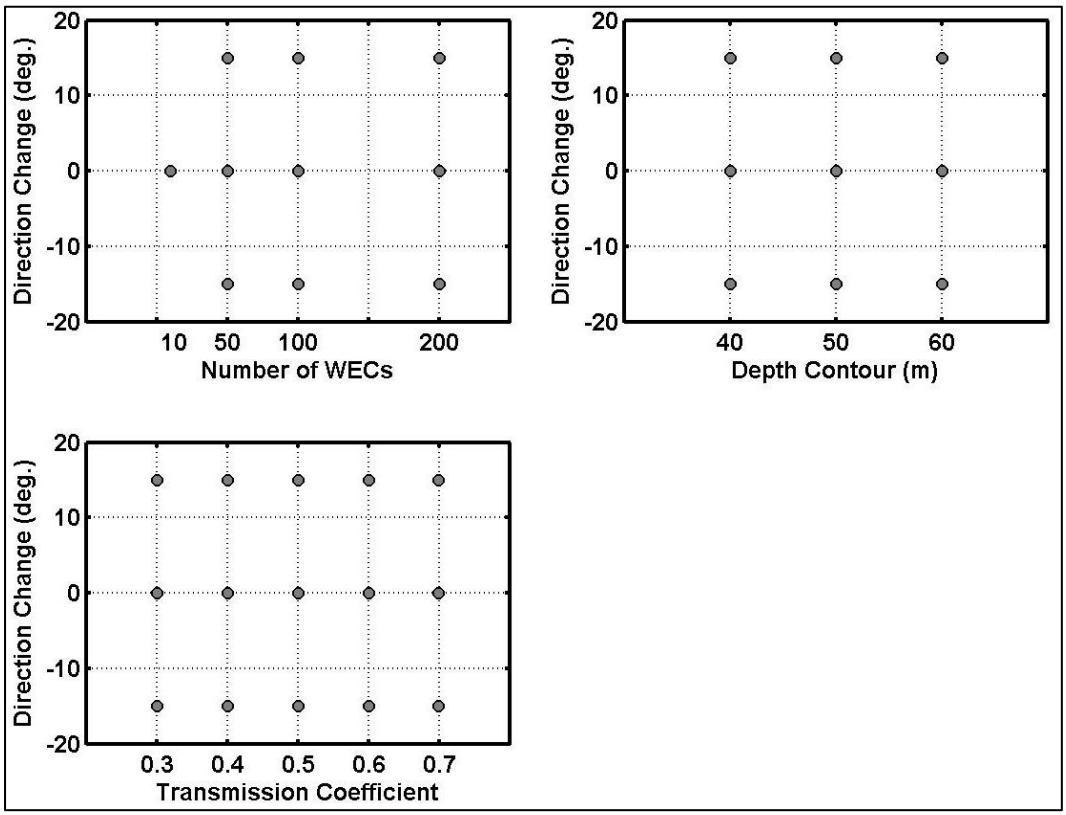

Figure 27. Variation in mean wave direction for all varied parameters.

These results ultimately illustrate, that, given the present model setup, the wave heights (and associated near-bottom orbital velocities) are most sensitive to the selected variables. Wave periods did not appear to be sensitive to changes in parameters; moreover, wave direction was not as sensitive to changes in the parameters, but did show some variation. However, additional analysis is required to fully explore the model sensitivity of peak wave period and mean wave direction to the varying of the parameters.

Model output locations located to the East and West showed relatively little to no change in wave heights compared to the baseline scenario. The largest wave height differences were observed downstream of the array near the array centerline (output locations 7-12), where the largest wave shadowing effects were predicted. Depending upon the parameters selected during each scenario, additional model output locations may also indicate large changes in wave heights (e.g. output locations such as 14-15, which are more affected by a large WEC array).

Conclusions

The presence of WEC arrays have the potential to significantly alter wave propagation patterns and affect coastal circulation patterns, sediment transport patterns, and alter ecosystem processes. To help accelerate deployment of environmentally friendly WEC arrays, predictive modeling tools must be developed to accurately represent WEC induced changes in wave propagation and evaluate the potential for environmental impact. The present study utilized an industry standard wave modeling tool, SWAN, to examine potential WEC array deployment scenarios at a site on the California coast and investigate model sensitivity so that the model can be effectively and confidently used in environmental studies. This analysis built upon a previous sensitivity analysis in which SWAN model parameters were varied to examine their effect on model results (SNL, 2011).

In the present study, model obstacle transmission coefficients were further investigated in conjunction with the number of WEC devices (obstacles) specified in an array, and the array deployment location (depth contour). The primary wave properties of interest (significant wave height, near-bottom orbital velocity, peak wave period, and mean wave direction) were investigated downstream of the array locations to evaluate overall near- and far-field effects of arrays on the wave properties in the region.

The sensitivity study illustrates that the wave heights are most sensitive to the variation in the parameters examined in this study. Locations in the lee centerline of the arrays in each modeled scenario showed the largest potential changes in wave height (and near-bottom orbital velocity) compared to those at the eastern and western fringes of the shadow zone. The largest wave height variation is realized when the transmission coefficient is lowest (0.3), the deployment location is the shallowest (40 m depth contour) and closest to shore, and the number of WEC devices in the array is the largest (200 devices). This scenario corresponds to the most wave energy “absorption”, shallowest array location and largest horizontal extent “disruption” of wave energy propagation (due to the large number of obstacles).

Both wave height and near-bottom orbital velocity are subject to the largest potential variations, each decreasing in sensitivity as transmission coefficient increases, as number of WEC devices decreases, and as the deployment location moves offshore. Wave direction is affected consistently for all parameters; and wave period is not affected (or negligibly affected) by varying parameters.

Generally, the changes in wave height are the primary alteration caused by the presence of a WEC array. Specifically, transmission coefficient variations directly result in wave height variations; however, it is important to utilize ongoing laboratory studies and future field tests to determine the most appropriate transmission coefficient values for a particular WEC device and configuration. Until transmission coefficient values can be accurately determined or WEC ‘friendly’ model enhancements are validated, this study shows that environmental assessments of WEC devices should focus on evaluating a range of transmission coefficients in order to determine the potential effects resulting from the presence of a WEC array.

The study results also indicate that further sensitivity analysis may be required to refine the model predictions and interpretations. Specifically,

- The frequency and directional bin spacing settings in the model should be minimized to more effectively evaluate the small-scale changes in wave period and direction resulting from WEC arrays.

- Frequency and directional spreading parameter variation, and their impact on downstream wave shadowing should be investigated further to determine the appropriate leeward distance at which a wave field "recovers" from the shadowing effects of WEC arrays.
- Multiple offshore incident wave angles should be examined to determine the likelihood of WEC array effects reaching shorelines.

References

Booij, N., Holthuijsen, L.H. and R.C. Ris, 1996, The SWAN wave model for shallow water, Proc. 25th Int. Conf. Coastal Engng., Orlando, USA, Vol. 1, pp. 668-676.

Chang, G and C. Jones, D. Hansen, M. Twardowski and A.. Barnard. 2010. Prediction of Optical Variability in Dynamic Near-shore Environments: Task Completion Report #3 – Numerical Modeling and Verification. 28 pp (unpublished).

Sandia National Laboratories. (2011). Investigation of Wave Energy Converter Effects on Wave Fields: A Modeling Sensitivity Study in Monterey Bay, CA. Water Power Technologies. Dec. 31, 2011.

Appendix A - Modeled Scenarios

Table A.1 List of model boundary conditions and scenarios (gray cells denote constants).

Run	Input Hs (m)	Input Tp (s)	Input MWD (deg)	Reflection Coefficient	Gamma – Freq Spreading	M – Dir Spreading (power)	Transmission Coefficient	# WEC Devices	Array Depth Contour(m)
1	1.7	12.5	205	0	3.3	10	0.3	10	40
2	1.7	12.5	205	0	3.3	10	0.4	10	40
3	1.7	12.5	205	0	3.3	10	0.5	10	40
4	1.7	12.5	205	0	3.3	10	0.6	10	40
5	1.7	12.5	205	0	3.3	10	0.7	10	40
6	1.7	12.5	205	0	3.3	10	0.3	50	40
7	1.7	12.5	205	0	3.3	10	0.4	50	40
8	1.7	12.5	205	0	3.3	10	0.5	50	40
9	1.7	12.5	205	0	3.3	10	0.6	50	40
10	1.7	12.5	205	0	3.3	10	0.7	50	40
11	1.7	12.5	205	0	3.3	10	0.3	100	40
12	1.7	12.5	205	0	3.3	10	0.4	100	40
13	1.7	12.5	205	0	3.3	10	0.5	100	40
14	1.7	12.5	205	0	3.3	10	0.6	100	40
15	1.7	12.5	205	0	3.3	10	0.7	100	40
16	1.7	12.5	205	0	3.3	10	0.3	200	40
17	1.7	12.5	205	0	3.3	10	0.4	200	40
18	1.7	12.5	205	0	3.3	10	0.5	200	40
19	1.7	12.5	205	0	3.3	10	0.6	200	40
20	1.7	12.5	205	0	3.3	10	0.7	200	40
21	1.7	12.5	205	0	3.3	10	0.3	10	50
22	1.7	12.5	205	0	3.3	10	0.4	10	50
23	1.7	12.5	205	0	3.3	10	0.5	10	50
24	1.7	12.5	205	0	3.3	10	0.6	10	50
25	1.7	12.5	205	0	3.3	10	0.7	10	50
26	1.7	12.5	205	0	3.3	10	0.3	50	50
27	1.7	12.5	205	0	3.3	10	0.4	50	50
28	1.7	12.5	205	0	3.3	10	0.5	50	50
29	1.7	12.5	205	0	3.3	10	0.6	50	50
30	1.7	12.5	205	0	3.3	10	0.7	50	50
31	1.7	12.5	205	0	3.3	10	0.3	100	50
32	1.7	12.5	205	0	3.3	10	0.4	100	50
33	1.7	12.5	205	0	3.3	10	0.5	100	50
34	1.7	12.5	205	0	3.3	10	0.6	100	50
35	1.7	12.5	205	0	3.3	10	0.7	100	50
36	1.7	12.5	205	0	3.3	10	0.3	200	50
37	1.7	12.5	205	0	3.3	10	0.4	200	50
38	1.7	12.5	205	0	3.3	10	0.5	200	50
39	1.7	12.5	205	0	3.3	10	0.6	200	50
40	1.7	12.5	205	0	3.3	10	0.7	200	50
41	1.7	12.5	205	0	3.3	10	0.3	10	60
42	1.7	12.5	205	0	3.3	10	0.4	10	60
43	1.7	12.5	205	0	3.3	10	0.5	10	60

44	1.7	12.5	205	0	3.3	10	0.6	10	60
45	1.7	12.5	205	0	3.3	10	0.7	10	60
46	1.7	12.5	205	0	3.3	10	0.3	50	60
47	1.7	12.5	205	0	3.3	10	0.4	50	60
48	1.7	12.5	205	0	3.3	10	0.5	50	60
49	1.7	12.5	205	0	3.3	10	0.6	50	60
50	1.7	12.5	205	0	3.3	10	0.7	50	60
51	1.7	12.5	205	0	3.3	10	0.3	100	60
52	1.7	12.5	205	0	3.3	10	0.4	100	60
53	1.7	12.5	205	0	3.3	10	0.5	100	60
54	1.7	12.5	205	0	3.3	10	0.6	100	60
55	1.7	12.5	205	0	3.3	10	0.7	100	60
56	1.7	12.5	205	0	3.3	10	0.3	200	60
57	1.7	12.5	205	0	3.3	10	0.4	200	60
58	1.7	12.5	205	0	3.3	10	0.5	200	60
59	1.7	12.5	205	0	3.3	10	0.6	200	60
60	2	12	310	0.5	3.3	10	0.7	200	60

Appendix B – Summary of Previous Model Sensitivity Analysis (SNL, 2011)

Model Setup

For this analysis, a 10-WEC device honeycomb array shape was selected as a representative configuration (Figure 28). Each WEC device was assumed to occupy a grid cell of approximately 25 meters. The WEC array was roughly centered on the 50 m depth contour southwest of Santa Cruz, CA. The array was oriented such that the broadest array dimension was perpendicular to the incident wave direction. The configuration utilized is a commonly proposed configuration for point absorbers. The setup yielded the most conservative estimate of changes in wave energy as a wider array footprint would "block" more wave energy from propagating past. Device separation distances evaluated during this evaluation included 2.5 diameter (2.5X), 5 diameter (5X) and 10 diameter (10X)spacing. Diameter spacing was selected to evaluate a range of array geometry while still being able to resolve individual WEC devices in the model grid resolution. The following sections describe the model setup and results of the sensitivity analysis. Sections have been abbreviated from the original report for brevity (SNL, 2011).

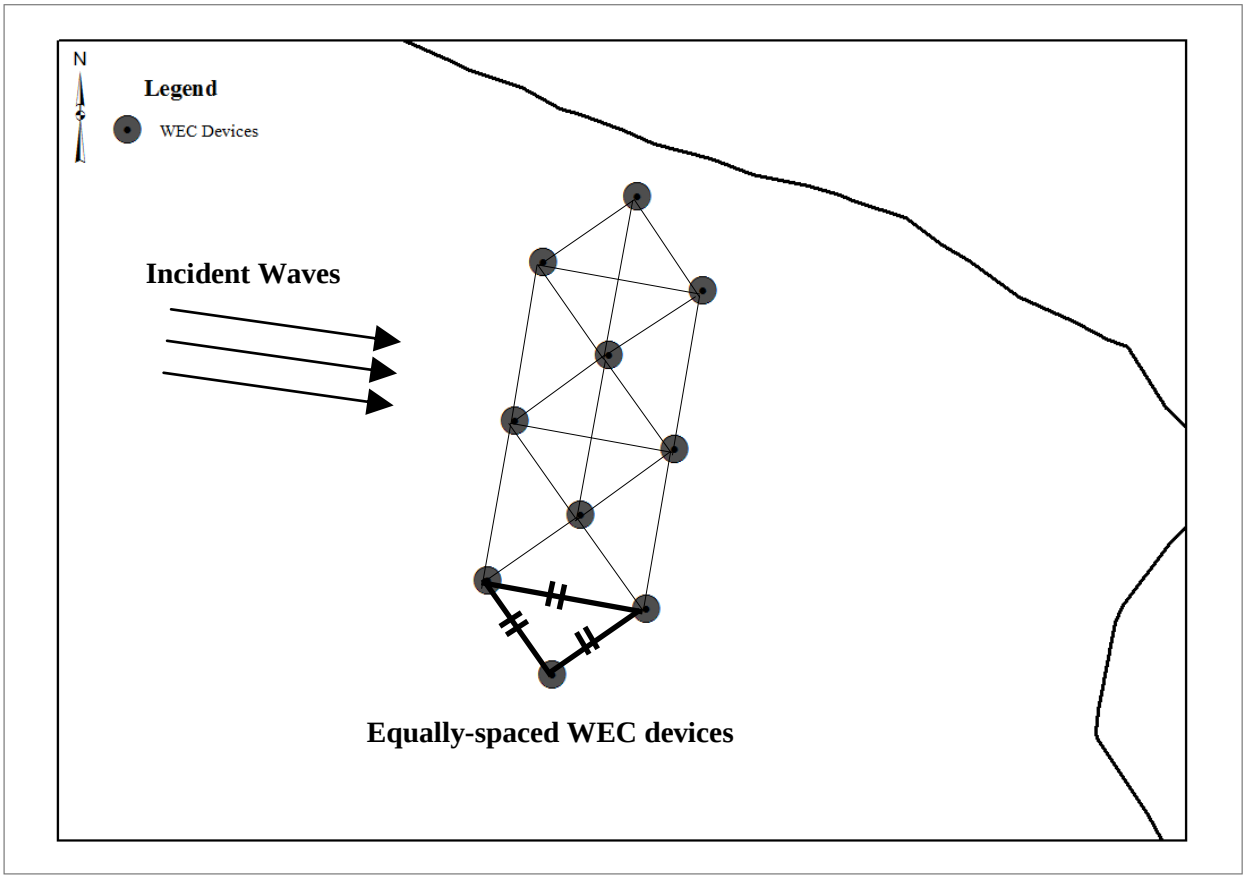

Figure 28. Honeycomb geometry of WEC device arrays in model. The 50 m depth contour is shown as a solid black line.

Boundary Conditions

The boundary wave conditions shown in Table 5 were selected for the model sensitivity analysis. They are a rough approximation of the values described in the Model Boundary Conditions section above, with consideration given to all three statistical parameters. The selected model input wave height (2.0 m) is the median value of the statistical data record. The model input wave period is

roughly the average of the 3 statistical parameters. The model input wave direction is the most frequently occurring direction from which the waves approach (mode) and also agrees roughly with the dominant wave period selection (12 seconds). This directional selection will be fixed for the modeling effort so incident waves will approach the broad side of the array perpendicularly.

Table 5. Model Boundary Conditions.

Parameter	Value
Hs (m)	2.0
Tp (sec)	12.0
MWD (degrees)	310

Model Domain

The Monterey Bay model domain is shown in Figure 29. The outer dashed outline denotes the Monterey Bay model domain; the inner dashed outline denotes the nested Santa Cruz model domain. The 50 m depth contour is illustrated as a thick black line; 40 meter and 60 meter depth contours are shown inshore and offshore of the 50 meter contour, respectively, as thin, black lines. The gray circle outline illustrates the location of the WEC array in the model.

Model boundary conditions were specified for all offshore "wet" boundaries (north, west and south sides of the domain). Offshore wave parameters are as listed in Table 2. Waves were propagated from offshore to onshore throughout the entire Monterey Bay domain. Wave frequency and directional spectra were extracted along the "wet" boundaries of the Santa Cruz domain and used as input boundary conditions for the nested, Santa Cruz domain (Figure 30).

Waves were then propagated from the offshore boundaries of the Santa Cruz domain to the shoreline. A baseline condition was modeled, in which no obstacles existed to block wave energy. Then, a condition that incorporated obstacles into the model was processed to ascertain the effects of the obstacles (WEC devices) on the wave conditions and the model sensitivity to varying wave conditions.

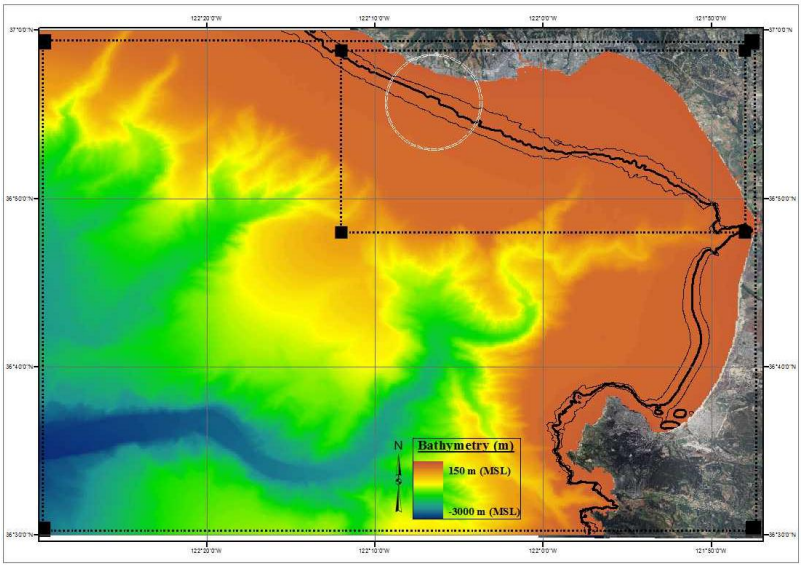

Figure 29. Monterey Bay model domain and nested Santa Cruz nested model domain (dashed box outline). Gray circle indicates WEC array location.

The WEC array was centered on the 50 meter depth contour, approximately. The broadest array face was oriented perpendicular to the 280 degree direction, the direction of normal wave incidence at that location given an offshore wave direction of 310 degrees. The wave direction rotation from that specified at the boundaries is a result of the effects of wave refraction.

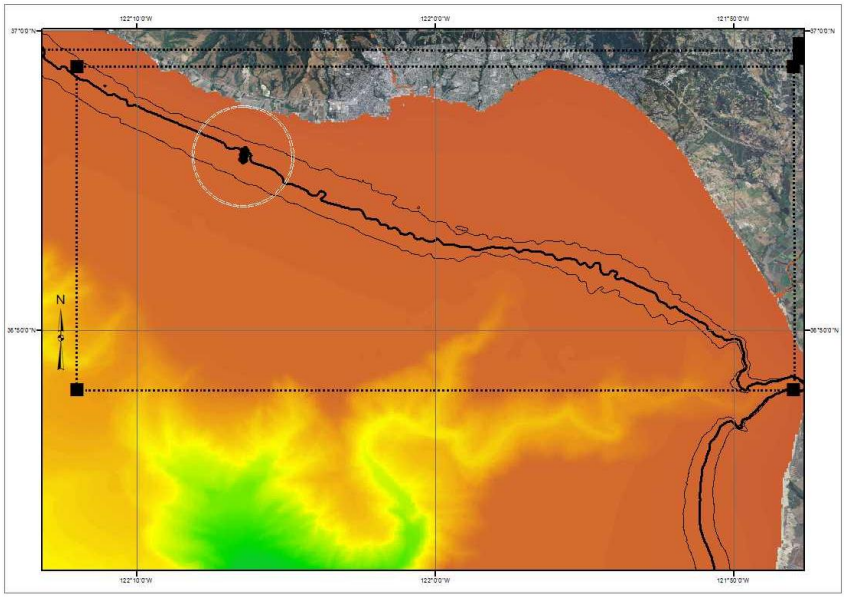

Figure 30. Nested Santa Cruz domain (dashed outline) with WEC device array shown (in gray circle).

In order to evaluate the effects of the array and associated parameters on the wave propagation, output was extracted from 15 locations during this evaluation (point descriptions are listed in Table 3 and displayed in Figure 31 and Figure 32). Eight locations surrounded the WEC arrays, each evenly spaced from the WEC array centerline. The spacing for all array geometries was arbitrarily selected to be twenty-five (25) times the WEC device diameters: 625 meters. This provided suitable model output locations for all array geometry spacing; output locations were the same for all array geometries to allow direct comparison of model predicted wave conditions.

Table 6. Model Output Locations and Descriptions.

Model Output Location	Description
1	Upstream – Offshore
2	Upstream – Centerline
3	Upstream – Onshore
4	Side – Offshore
5	Side – Onshore
6	Downstream – Offshore
7	Downstream – Centerline
8	Downstream – Onshore
9	Downstream – Centerline 1 km
10	Downstream – Centerline 5 km
11	Downstream – Centerline 10 km
12	Downstream – Centerline 20 km
13	Nearshore – Point Santa Cruz
14	Nearshore – Santa Cruz Beach
15	Nearshore – Pleasure Point

Four additional output locations were located 1 km, 5 km, 10 km and 20 km directly downstream of the center of the WEC array. Three near-shore locations were sited offshore of Point Santa Cruz (west of the wharf structure in 15 meters water depth), Santa Cruz beach (in 6 meters of water depth), and offshore of Pleasure Point (east of the wharf structure in 6 meters water depth). These are popular surfing locations, with surf breaks extending all the way around the points into the beaches at Santa Cruz. Changes in wave conditions due to the WEC array, if any, are important to ascertain at this location since this will concern the surfing community. Furthermore, changes in wave conditions at this near-shore location are important to evaluate from a shoreline erosion perspective.

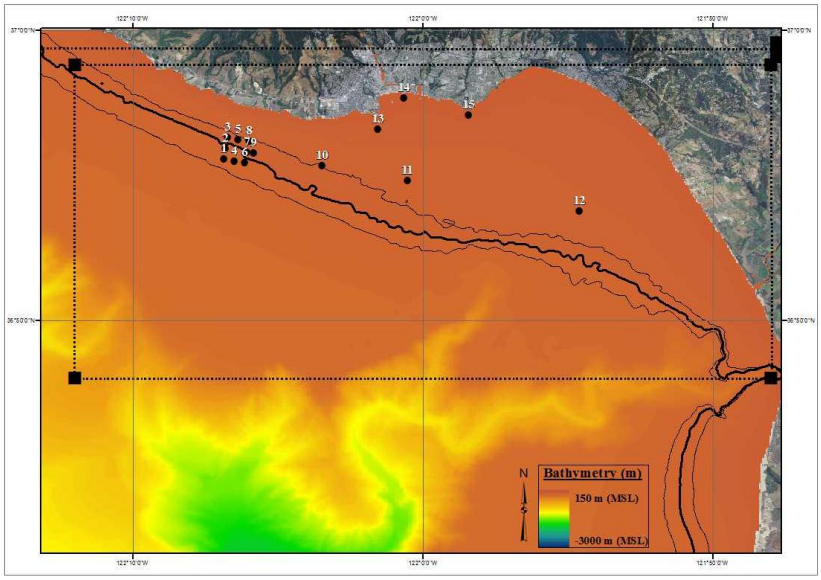

Figure 31. Nested Santa Cruz domain showing model output locations.

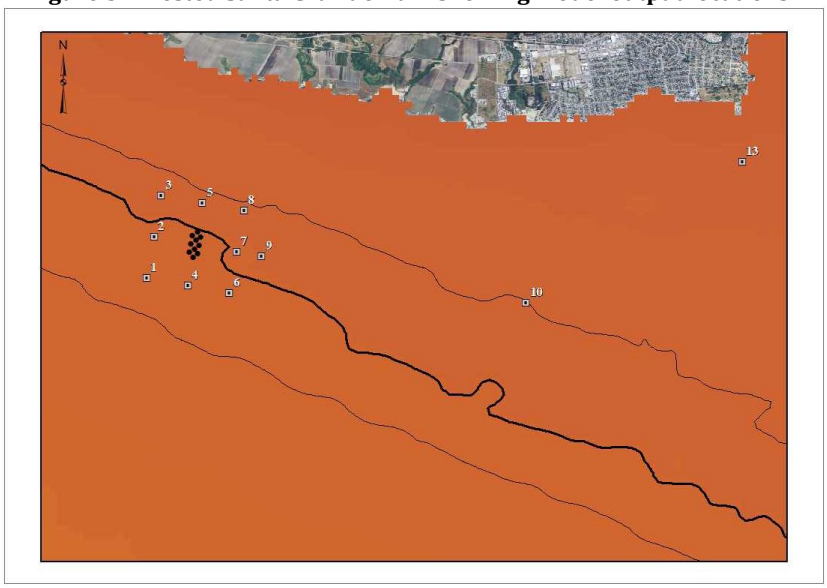

Figure 32. Expanded view of WEC device array (black dots) and model output locations in proximity.

Model Parameters

The Monterey Bay and Santa Cruz model domains were used to conduct a model sensitivity analysis, to determine the changes in model predictions for particular obstacle reflection and transmission coefficients. Specifically, one objective was to evaluate the changes in wave height, period and direction resulting from the WEC devices and array based on user-input, frequency-independent coefficients.

Within SWAN, reflection and transmission coefficients determine the amount of wave energy that is reflected by the obstacles or allowed to transmit past the obstacles. By varying these values, the effect of the WEC devices reflection and absorption can be quantified.

In addition, the frequency and directional spreading coefficients were varied within the sensitivity analysis. Narrow-banded frequency and directional spectra are akin to focused swell conditions (which are desired wave conditions by surfers). Wide-banded frequency and/or directional spectra are typically more common, and may indicate swell approaching from different directions; or may indicate the superposition of swell and locally generated wind-waves that are each approaching from different directions.

SWAN allows the user to select from two different methods of implementing obstacles: 1) a basic representation using a constant transmission coefficient and 2) a more complex representation of simulating the obstacle as a dam, whereby the transmission coefficient depends upon the incident wave conditions and the obstacle height. Both methods allow a reflection coefficient to also be specified (to represent reflected wave energy). The latter method requires additional coefficient specifications based upon published methods of computing wave energy transmission. These additional specifications are not described in this memorandum.

For this study, the former method of defining the transmission coefficient (constant transmission and reflection coefficients) was selected for simplicity of evaluating the model sensitivity. The parameter value ranges used in the sensitivity analysis are listed in Table 4.

Table 7. Sensitivity analysis parameter values.

Coefficient	Value(s)
Transmission	[0.00, 0.25, 0.50, 0.75, 1.00]
Reflection	[0.00, 0.25, 0.50]
Frequency Spreading (gamma)	[1.0, 3.3, 10.0]
Directional Spreading (m)	[2.0, 10.0, 25.0]

Results and Discussion

Comparisons to Baseline Scenario

Results included propagated wave heights, wave periods and wave directions at all grid points in the domain, as well as other computed quantities such as energy dissipation and bottom wave orbital velocities. Figure 33-Figure 36 display example wave height predictions from a baseline condition (no WEC devices) and 3 non-baseline conditions (incorporating WEC devices: 2.5X, 5X, and 10X WEC device spacing, respectively). Figure 37 is an expanded view of the wave height predictions at the WEC 5X spacing array that illustrates the wave height decreases in the lee as a result of "blocked" wave energy. All scenarios shown were modeled with the parameters listed for Run #8 in Table Appendix.1: a transmission coefficient of 0.0 (wave energy completely blocked at WEC device), a reflection coefficient of 0.0 (no wave energy reflection at WEC device), a frequency spreading coefficient of 10 ("peakier" spectral shape representative of swell conditions) and a directional spreading coefficient of 10 (narrow spreading, more focused waves).

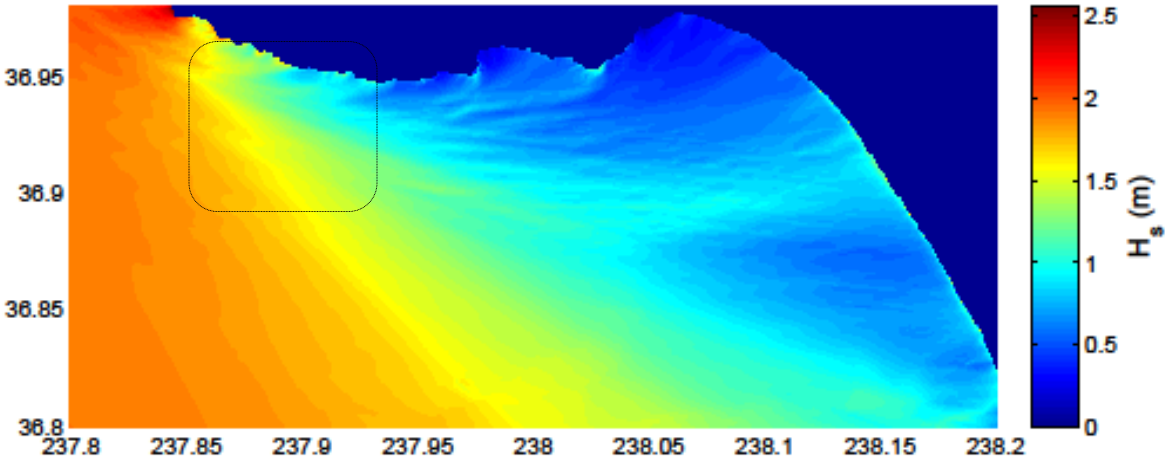

Figure 33. Model wave height results from BASE condition. Dashed outline indicates location where

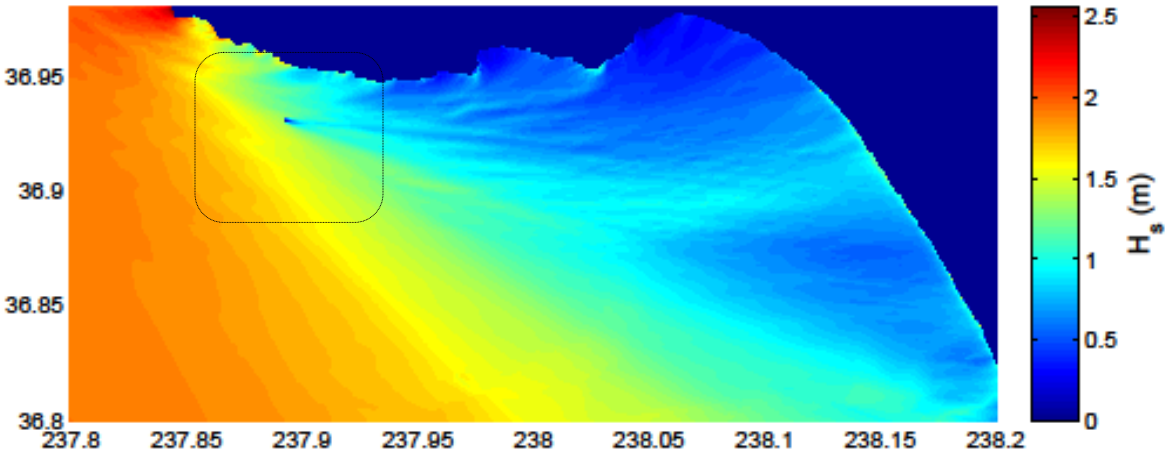

Figure 34. Model wave height results from 2.5X spacing ARRAY condition.

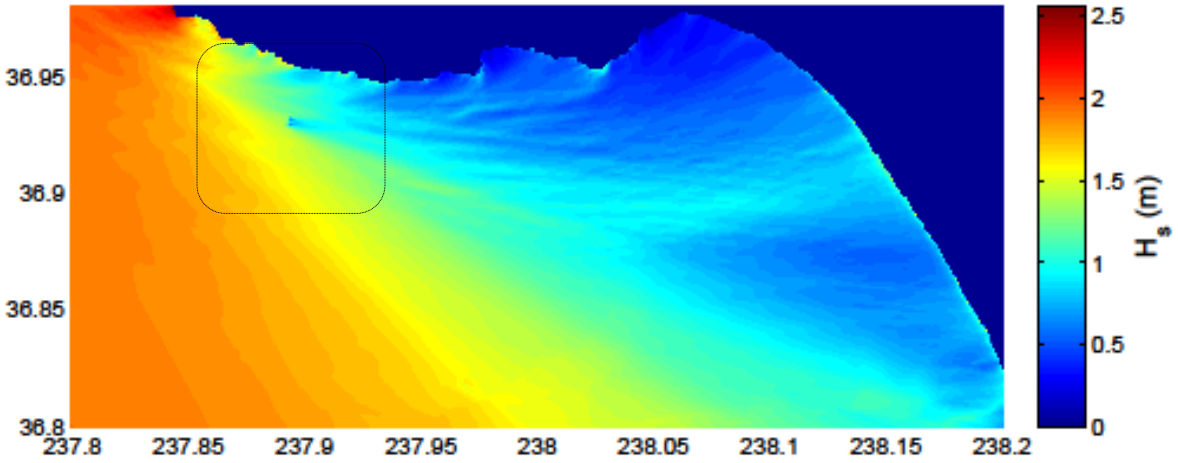

Figure 35. Model wave height results from 5X spacing ARRAY condition.

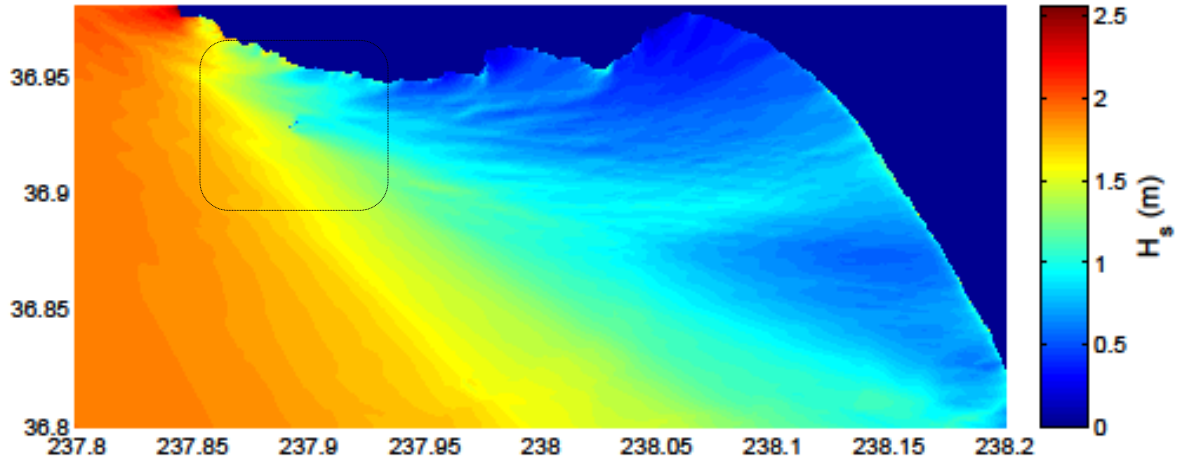

Figure 36. Model wave height results from 10X spacing ARRAY condition.

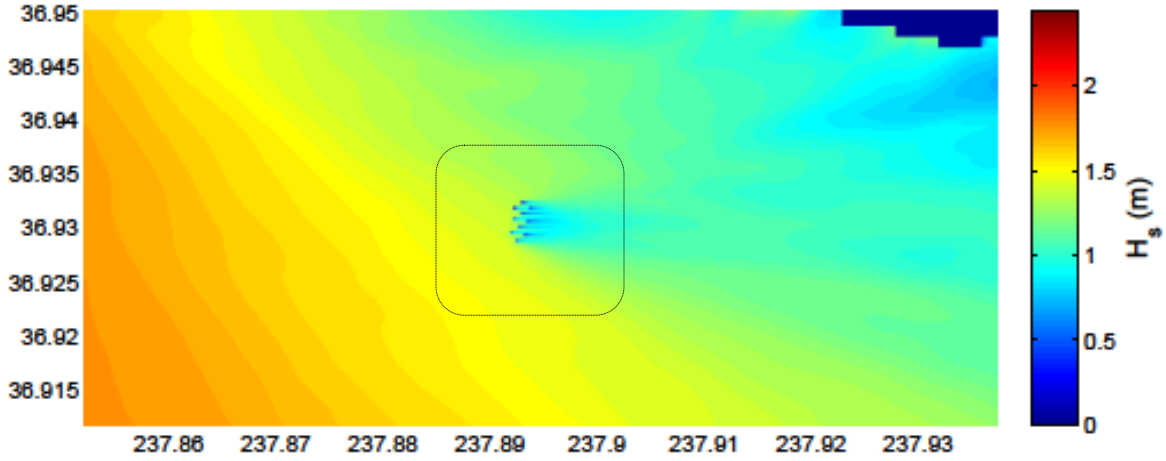

Figure 37. Expanded view of model wave height results from 5X spacing ARRAY condition.

Immediately evident from examination of Figure 33-Figure 36 is that array device spacing has an effect on downstream wave conditions, both near-field and far-field. Based on visual observation, closer spacing of WEC devices (e.g. 2.5X) will result in a larger decrease in wave energy propagation near the array compared to larger spaced arrays (5X or 10X spacing); The far-field effect of a closer-spaced array on the wave conditions is not as significant as larger-spaced arrays. However, to truly evaluate the far-field effects of the device spacing, the differences in wave conditions at the model output locations needs to be quantified.

To facilitate this, the model output wave heights, wave periods and wave directions from each model run (and each array device spacing geometry) were compared individually to the baseline scenario model predictions. One at a time, the four sensitivity variables were held constant while the others were allowed to vary. The resulting differences in each wave condition were plotted for observation.

Figure 38 is an example scatter plot of percentage wave height differences at model output location 7 (downstream centerline of the array). Negative percentage indicates a wave height that has decreased in value from the baseline scenario value (due to absorbed, reflected or blocked wave energy). Each subplot denotes the model scatter that results from holding a particular sensitivity

parameter constant while allowing the remaining parameters to vary. Clockwise from the top left, the sensitivity parameters held constant in each subplot are: transmission coefficient, reflection coefficient, directional spreading factor and the frequency spreading factor.

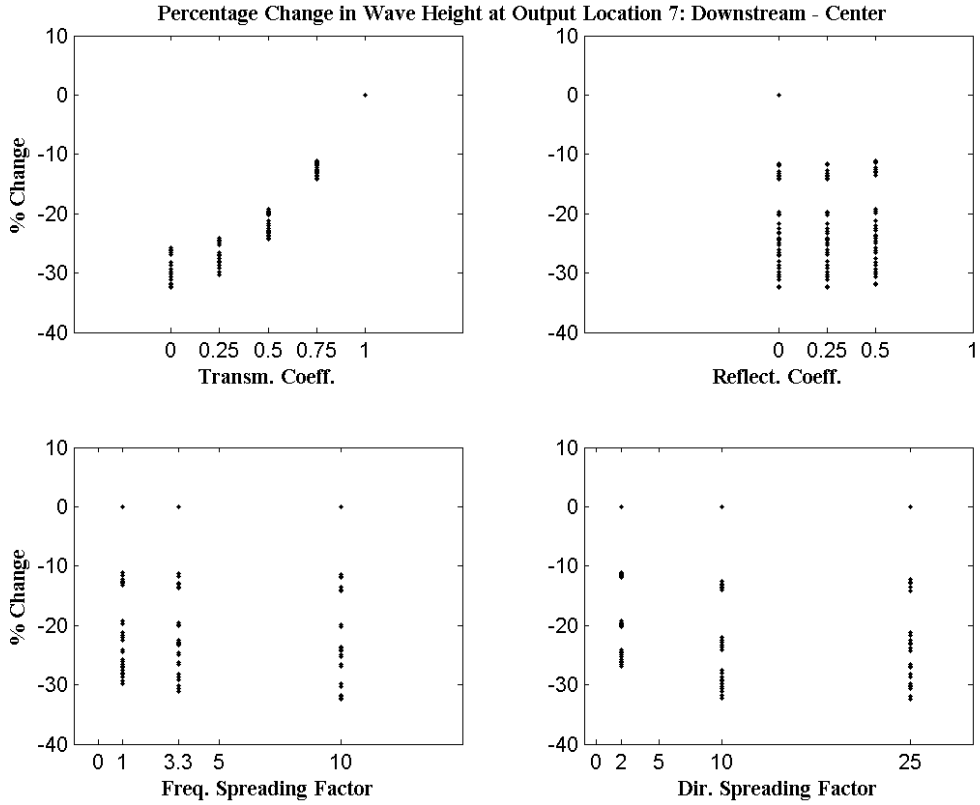

Figure 38. Sensitivity analysis scatter plot for the 5X device spacing and model output location 7: Downstream Centerline. Each subplot represents a sensitivity analysis for a constant variable.

The shape of the resulting scatter plot and degree of vertical spreading that exists for each constant parameter are indications of the model sensitivity to that parameter. For example, setting the transmission coefficient to zero (in the top left subplot) and allowing all other sensitivity parameters to vary results in a minimum decrease in wave height of ~25% and a maximum decrease in wave height of ~35% (vertical maximum and minimum for a transmission coefficient equal to 0).

On the other hand, by holding the frequency spreading factor constant to 1, 3.3 or 10 (bottom left plot), a wide range of values results, from a 0% to ~30% decrease in wave height at this location, irrespective of the value of frequency spreading parameter chosen. This indicates that the model results are not very sensitive to the selected frequency spreading factor. In other words, the other varying parameters (e.g. transmission coefficient) has a much large effect on wave heights.

Figure 38 ultimately illustrates that the model results are most sensitive to the transmission coefficient at this downstream location. Similar evaluations were made for the wave periods and wave directions modeled at each output location (these figures are shown in the appendices). In general, wave period decreases were also sensitive to the transmission coefficient, and, to a lesser degree, the directional spreading factor (lower directional spreading coefficient resulted in less scatter in model prediction). Wave direction was not as sensitive to changes in the coefficients as

the other wave parameters (changes were small or negligible between baseline and array scenarios). Some changes were observed; however, additional analysis is required to fully explain the model sensitivity of mean wave direction to the varying of the parameters.

To summarize, model output locations upstream and to the sides of the array showed little to no change in wave heights compared to the baseline scenario. The largest wave height differences were observed downstream of the array along the array centerline (output locations 7 and 9). As distance downstream of the array increases (output locations 10-12), wave height percentage change decreases in magnitude, as the effects of wave energy absorption and diffraction are mitigated.

Wave period changes at most model output locations were negligible (less than 0.5%). At nearby downstream array centerline locations, however, wave period decreased up to 8% from the baseline scenario. This amounts to a 1 second decrease in wave period for a 12 second incident wave and may be more of a result of the frequency bin spacing selected for model input than a decrease in wave period. Further evaluation is needed to full explain the decrease in wave periods resulting from wave energy absorption.

Wave directional changes were also largely negligible (zero change) at most model output locations. For the downstream centerline locations, however, wave direction decreased up to 15 degrees (counterclockwise rotation of wave direction). The reason for this is not immediately clear and may be a result of several factors: natural wave refraction combined with a large directional spreading parameter in the wave spectrum. Furthermore, it may also be a consequence of the directional bin spacing selected for model input.

Comparisons to Different WEC Device Spacing

Similar comparisons were made between different WEC device array spacings to identify the effect the spacings have on both near- and far-field wave conditions. Figure 39 illustrates the percentage change in wave height between the 10X spacing and 2.5X spacing arrays at model location 7. In addition, the percentage change in wave height at model output location 10, downstream 5 km, is shown in Figure 40. A negative percentage means that the 10X case has a lesser effect on wave heights than the 2.5X by the negative percentage listed.

The distance effects of wave energy shadowing are evident upon comparison of these figures. A more closely spaced array blocks a large amount of wave energy at the array location, causing a large decrease in wave height in the immediate lee of the array. The wave energy downstream disperses rapidly, however, so far-field shadowing of wave height (e.g. greater than 5 km distant) is not observed. For larger spaced arrays, the wave energy may not be blocked as much in the near-field, but the effects propagate much further downstream: the wave field does not recover from the energy loss as rapidly.

Comparisons were made between all array spacings evaluated in this study: 10X: 2.5X, 10X:5X, and 5X to 2.5X). The largest differences in wave height are observed when comparing the 10X to 2.5X spacing. At output location 7, when the transmission coefficient is zero (most conservative), wave heights in the lee of the smaller spaced array are 10-25% smaller than those in the lee of the larger spaced array. The wave height decreases between 10X and 5X spacing at model output location 7 are not as large, varying between 10% and 20% for a transmission coefficient of 0. The wave height decrease between 5X and 2.5X is even smaller, varying between 0% and 10% for a transmission coefficient of 0.For comparison, at model output location 10, when the transmission coefficient is zero, wave heights in the lee of the smaller spaced array are up to 5% larger than those in the lee of

the larger spaced array. This is a strong indication that the larger spaced array is still causing shadowing effects of the wave energy at this output location.

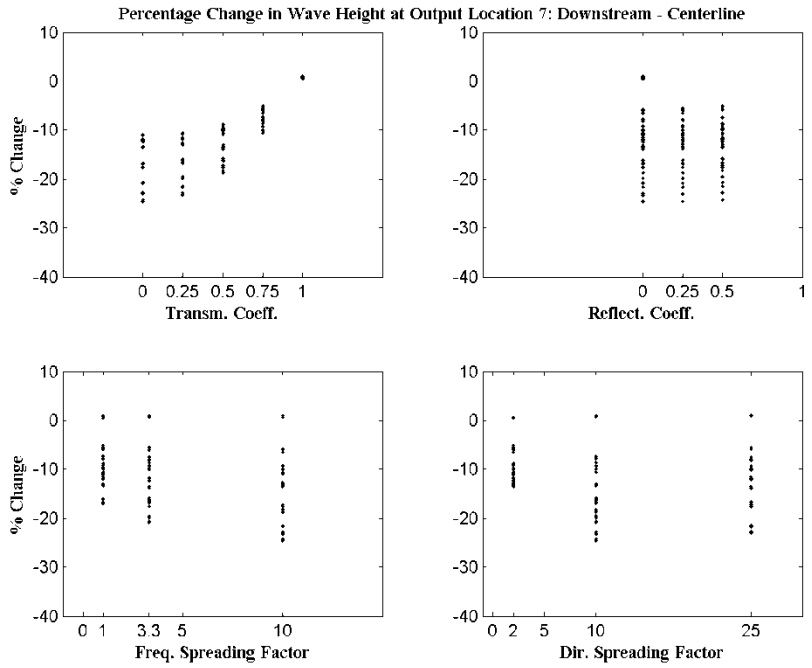

Figure 39. Sensitivity analysis scatter plot for 10X to 2.5X spacing comparison at model output location 7: Downstream Centerline. The Y-axis is percent change in wave heights between 10X and 2.5X spacing.

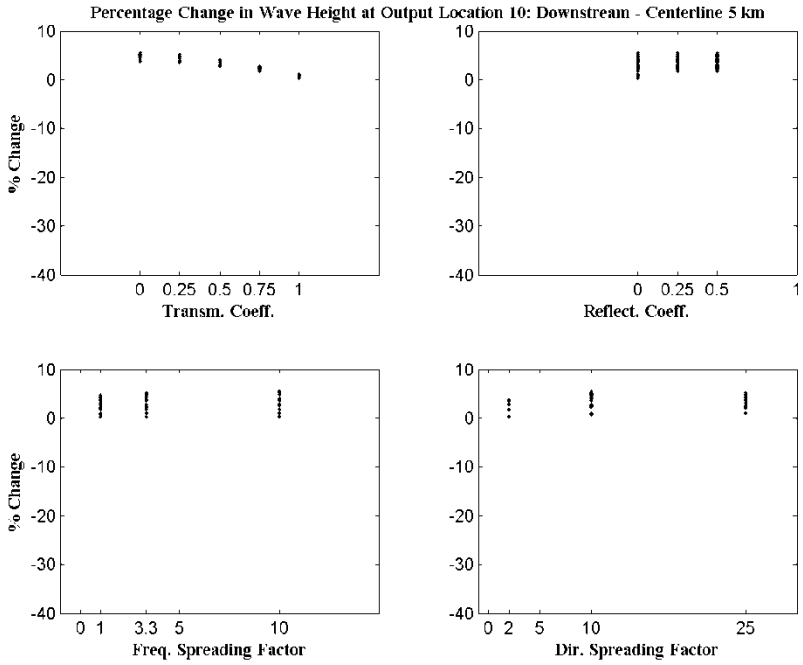

Figure 40. Sensitivity analysis scatter plot for 10X to 2.5X spacing comparison at model output location 10: Downstream 5 km. The Y-axis is percent change in wave heights between 10X and 2.5X spacing.

Conclusions

The presence of WEC arrays have the potential to alter wave propagation patterns significantly and affect coastal circulation patterns, sediment transport patterns, and alter ecosystem processes. Since no arrays have been installed at a real world site yet, we must rely on predictive modeling tools to develop the ranges of anticipated scenarios and evaluate the potential for environmental impact. The present study utilizes an industry standard wave modeling tool, SWAN, to examine a proposed wave array deployment at a site on the California coast and investigate model sensitivity so that the model can be effectively and confidently used in environmental studies.

The primary wave properties of interest (height, period, and direction) were investigation in the vicinity of the arrays to evaluate overall effects of arrays on waves in the region. The model output locations upstream and to the sides of the array showed little to no change in wave heights compared to the baseline scenario. The largest wave height differences were observed downstream of the array along the array centerline. As distance downstream of the array increases (output locations 10-12), wave height percentage change decreases in magnitude, as the effects of wave energy absorption and diffraction become negligible. Wave period and directional changes at most model output locations were generally negligible. A few cases showed minimal change which will be investigated in more focused environmental studies.

The sensitivity study illustrates that the wave heights are most sensitive to the transmission coefficient and that the other model parameters have a minimal effect on overall change in wave height. Similar evaluations were made for the wave period and wave direction sensitivity to model parameters. In general, wave period decreases were also sensitive to the transmission coefficient, and, to a lesser degree, the directional spreading factor (lower directional spreading coefficient resulted in less scatter in model prediction). Wave direction was not as sensitive to changes in the coefficients as the other wave parameters (changes were small or negligible between baseline and array scenarios). Some changes were observed; however, additional analysis is required to fully explain the model sensitivity of mean wave direction to the varying of the parameters.

The study found that array device spacing has an effect on downstream wave conditions, both near-field and far-field. Based on visual observation, closer spacing of WEC devices (e.g. 2.5X) will result in a larger decrease in wave energy propagation near the array compared to larger spaced arrays (5X or 10X spacing); The far-field effect of a closer-spaced array on the wave conditions is not as significant as larger-spaced arrays.

Generally, the changes in wave height are the primary alteration resulting in the presence of a WEC array. Since the transmission coefficient is shown to generate the largest sensitivity, it is important to utilize ongoing laboratory studies and future field tests to determine the most appropriate values for a particular WEC device. Until those values can be accurately determined, this study shows that environmental assessments of WEC devices should focus on evaluating a range of transmission coefficients in order to determine the potential effects resulting from the presence of a WEC array. It appears that reasonable ranges of directional spreading coefficients have minimal effects on the overall results. Additionally, the spacing of an array has a significant effect on downstream wave properties.

Appendix

Model Sensitivity Parameters Used(SNL, 2011)

Table Appendix.1 List of parameter values used for sensitivity analysis.

Run	Input Hs (m)	Input Tp (s)	Input MWD (deg)	TransmCoeff	Reflect Coeff	Gamma – Freq Spreading	M – Dir Spreading
1	2	12	310	0.00	0.00	1.00	2.00
2	2	12	310	0.00	0.00	1.00	10.00
3	2	12	310	0.00	0.00	1.00	25.00
4	2	12	310	0.00	0.00	3.30	2.00
5	2	12	310	0.00	0.00	3.30	10.00
6	2	12	310	0.00	0.00	3.30	25.00
7	2	12	310	0.00	0.00	10.00	2.00
8	2	12	310	0.00	0.00	10.00	10.00
9	2	12	310	0.00	0.00	10.00	25.00
10	2	12	310	0.00	0.25	1.00	2.00
11	2	12	310	0.00	0.25	1.00	10.00
12	2	12	310	0.00	0.25	1.00	25.00
13	2	12	310	0.00	0.25	3.30	2.00
14	2	12	310	0.00	0.25	3.30	10.00
15	2	12	310	0.00	0.25	3.30	25.00
16	2	12	310	0.00	0.25	10.00	2.00
17	2	12	310	0.00	0.25	10.00	10.00
18	2	12	310	0.00	0.25	10.00	25.00
19	2	12	310	0.00	0.50	1.00	2.00
20	2	12	310	0.00	0.50	1.00	10.00
21	2	12	310	0.00	0.50	1.00	25.00
22	2	12	310	0.00	0.50	3.30	2.00
23	2	12	310	0.00	0.50	3.30	10.00
24	2	12	310	0.00	0.50	3.30	25.00
25	2	12	310	0.00	0.50	10.00	2.00
26	2	12	310	0.00	0.50	10.00	10.00
27	2	12	310	0.00	0.50	10.00	25.00
28	2	12	310	0.25	0.00	1.00	2.00
29	2	12	310	0.25	0.00	1.00	10.00
30	2	12	310	0.25	0.00	1.00	25.00
31	2	12	310	0.25	0.00	3.30	2.00
32	2	12	310	0.25	0.00	3.30	10.00
33	2	12	310	0.25	0.00	3.30	25.00
34	2	12	310	0.25	0.00	10.00	2.00
35	2	12	310	0.25	0.00	10.00	10.00
36	2	12	310	0.25	0.00	10.00	25.00
37	2	12	310	0.25	0.25	1.00	2.00
38	2	12	310	0.25	0.25	1.00	10.00
39	2	12	310	0.25	0.25	1.00	25.00
40	2	12	310	0.25	0.25	3.30	2.00
41	2	12	310	0.25	0.25	3.30	10.00
42	2	12	310	0.25	0.25	3.30	25.00
43	2	12	310	0.25	0.25	10.00	2.00

44	2	12	310	0.25	0.25	10.00	10.00
45	2	12	310	0.25	0.25	10.00	25.00
46	2	12	310	0.25	0.50	1.00	2.00
47	2	12	310	0.25	0.50	1.00	10.00
48	2	12	310	0.25	0.50	1.00	25.00
49	2	12	310	0.25	0.50	3.30	2.00
50	2	12	310	0.25	0.50	3.30	10.00
51	2	12	310	0.25	0.50	3.30	25.00
52	2	12	310	0.25	0.50	10.00	2.00
53	2	12	310	0.25	0.50	10.00	10.00
54	2	12	310	0.25	0.50	10.00	25.00
55	2	12	310	0.50	0.00	1.00	2.00
56	2	12	310	0.50	0.00	1.00	10.00
57	2	12	310	0.50	0.00	1.00	25.00
58	2	12	310	0.50	0.00	3.30	2.00
59	2	12	310	0.50	0.00	3.30	10.00
60	2	12	310	0.50	0.00	3.30	25.00
61	2	12	310	0.50	0.00	10.00	2.00
62	2	12	310	0.50	0.00	10.00	10.00
63	2	12	310	0.50	0.00	10.00	25.00
64	2	12	310	0.50	0.25	1.00	2.00
65	2	12	310	0.50	0.25	1.00	10.00
66	2	12	310	0.50	0.25	1.00	25.00
67	2	12	310	0.50	0.25	3.30	2.00
68	2	12	310	0.50	0.25	3.30	10.00
69	2	12	310	0.50	0.25	3.30	25.00
70	2	12	310	0.50	0.25	10.00	2.00
71	2	12	310	0.50	0.25	10.00	10.00
72	2	12	310	0.50	0.25	10.00	25.00
73	2	12	310	0.50	0.50	1.00	2.00
74	2	12	310	0.50	0.50	1.00	10.00
75	2	12	310	0.50	0.50	1.00	25.00
76	2	12	310	0.50	0.50	3.30	2.00
77	2	12	310	0.50	0.50	3.30	10.00
78	2	12	310	0.50	0.50	3.30	25.00
79	2	12	310	0.50	0.50	10.00	2.00
80	2	12	310	0.50	0.50	10.00	10.00
81	2	12	310	0.50	0.50	10.00	25.00
82	2	12	310	0.75	0.00	1.00	2.00
83	2	12	310	0.75	0.00	1.00	10.00
84	2	12	310	0.75	0.00	1.00	25.00
85	2	12	310	0.75	0.00	3.30	2.00
86	2	12	310	0.75	0.00	3.30	10.00
87	2	12	310	0.75	0.00	3.30	25.00
88	2	12	310	0.75	0.00	10.00	2.00
89	2	12	310	0.75	0.00	10.00	10.00
90	2	12	310	0.75	0.00	10.00	25.00
91	2	12	310	0.75	0.25	1.00	2.00

92	2	12	310	0.75	0.25	1.00	10.00
93	2	12	310	0.75	0.25	1.00	25.00
94	2	12	310	0.75	0.25	3.30	2.00
95	2	12	310	0.75	0.25	3.30	10.00
96	2	12	310	0.75	0.25	3.30	25.00
97	2	12	310	0.75	0.25	10.00	2.00
98	2	12	310	0.75	0.25	10.00	10.00
99	2	12	310	0.75	0.25	10.00	25.00
100	2	12	310	0.75	0.50	1.00	2.00
101	2	12	310	0.75	0.50	1.00	10.00
102	2	12	310	0.75	0.50	1.00	25.00
103	2	12	310	0.75	0.50	3.30	2.00
104	2	12	310	0.75	0.50	3.30	10.00
105	2	12	310	0.75	0.50	3.30	25.00
106	2	12	310	0.75	0.50	10.00	2.00
107	2	12	310	0.75	0.50	10.00	10.00
108	2	12	310	0.75	0.50	10.00	25.00
109	2	12	310	1.00	0.00	1.00	2.00
110	2	12	310	1.00	0.00	1.00	10.00
111	2	12	310	1.00	0.00	1.00	25.00
112	2	12	310	1.00	0.00	3.30	2.00
113	2	12	310	1.00	0.00	3.30	10.00
114	2	12	310	1.00	0.00	3.30	25.00
115	2	12	310	1.00	0.00	10.00	2.00
116	2	12	310	1.00	0.00	10.00	10.00
117	2	12	310	1.00	0.00	10.00	25.00